A Novel Disease Gene for Brugada Syndrome

Sarcolemmal Membrane–Associated Protein Gene Mutations Impair Intracellular Trafficking of hNav1.5

Taisuke Ishikawa, DVM*; Akinori Sato, MD, PhD*; Cherisse A. Marcou, BA; David J. Tester, BS; Michael J. Ackerman, MD, PhD; Lia Crotti, MD, PhD; Peter J. Schwartz, MD; Young Keun On, MD; Jeong-Euy Park, MD; Kazufumi Nakamura, MD, PhD; Masayasu Hiraoka, MD, PhD; Kiyoshi Nakazawa, MD, PhD; Harumizu Sakurada, MD, PhD; Takuro Arimura, DVM, PhD; Naomasa Makita, MD, PhD; Akinori Kimura, MD, PhD

Background—Mutations in genes including *SCN5A* encoding the α-subunit of the cardiac sodium channel (hNav1.5) cause Brugada syndrome via altered function of cardiac ion channels, but more than two-thirds of Brugada syndrome remains pathogenetically elusive. T-tubules and sarcoplasmic reticulum are essential in excitation of cardiomyocytes, and sarcolemmal membrane-associated protein (SLMAP) is a protein of unknown function localizing at T-tubules and sarcoplasmic reticulum.

Methods and Results—We analyzed 190 unrelated Brugada syndrome patients for mutations in *SLMAP*. Two missense mutations, Val269Ile and Glu710Ala, were found in heterozygous state in 2 patients but were not found in healthy individuals. Membrane surface expression of hNav1.5 in the transfected cells was affected by the mutations, and silencing of mutant *SLMAP* by small interfering RNA rescued the surface expression of hNav1.5. Whole-cell patch-clamp recordings of hNav1.5-expressing cells transfected with mutant *SLMAP* confirmed the reduced hNav1.5 current.

Conclusions—The mutations in *SLMAP* may cause Brugada syndrome via modulating the intracellular trafficking of hNav1.5 channel. (***Circ Arrhythm Electrophysiol*. 2012;5:1098-1107.**)

Key Words: arrhythmia mechanisms ■ genes ■ ion channels ■ sarcoplasmic reticulum

Brugada syndrome (BrS) is a cardiac channelopathy characterized by specific findings in the ECG such as accentuated J-wave and ST-segment elevation in the right precordial leads, which is often accompanied by syncope and sudden cardiac death attributable to ventricular arrhythmias.[1,2] Worldwide prevalence of BrS is ≈1 in 10 000, but it is much higher in Asian countries, reaching 5 to 10 in 10 000.[3–5] Approximately one-third of BrS patients have a family history of BrS and sudden cardiac death, which is consistent with the autosomal-dominant inheritance, suggesting that genetic abnormalities cause BrS.[6]

Clinical Perspective on p 1107

Mutations in 12 different genes have been reported in BrS.[7–13] The major disease gene for BrS is *SCN5A* that encodes the pore-forming α-subunit of the cardiac sodium channel hNav1.5; the *SCN5A* mutations reduce the availability of sodium channels, leading to the diminished peak of inward sodium current (I_{Na}) and the voltage-dependent shift in activation or inactivation profile attributable to the structural changes in the channel molecule or from trafficking abnormalities.[14,15] Mutations in genes encoding auxiliary

Received December 16, 2011; accepted September 13, 2012.

From the Department of Molecular Pathogenesis, Medical Research Institute, Tokyo Medical and Dental University, Tokyo, Japan (T.I., A.S., T.A., A.K.); Division of Cardiology, Niigata University Graduate School of Medical and Dental Sciences, Niigata, Japan (A.S.); Departments of Medicine (Division of Cardiovascular Diseases), Pediatrics (Division of Pediatric Cardiology), and Molecular Pharmacology and Experimental Therapeutics, Windland Smith Rice Sudden Death Genomics Laboratory, Mayo Clinic, Rochester, MN (C.A.M., D.J.T., M.J.A.); Institute of Human Genetics, Helmholtz Center Munich, Neuherberg, Germany (L.C.); Department of Molecular Medicine, Section of Cardiology, University of Pavia, Pavia, Italy (L.C., P.J.S.); Department of Cardiology, Fondazione IRCCS Policlinico S. Matteo, Pavia, Italy (L.C., P.J.S.); Cardiovascular Genetics Laboratory, Hatter Institute for Cardiovascular Research, Department of Medicine, University of Cape Town, Cape Town, South Africa (P.J.S.); Department of Medicine, University of Stellenbosch, Stellenbosch, South Africa (P.J.S.); Chair of Sudden Death, Department of Family and Community Medicine, College of Medicine, King Saud University, Riyadh, Saudi Arabia (P.J.S.); Division of Cardiology, Samsung Medical Center, Sungkyunkwan University School of Medicine, Seoul, Korea (Y.K.); Department of Cardiovascular Medicine, Okayama University Graduate School of Medicine, Dentistry and Pharmaceutical Sciences, Okayama, Japan (K.N.); Department of Cardiovascular Medicine, Medical Research Institute, Tokyo Medical and Dental University, Tokyo, Japan (M.H.); Division of Internal Medicine, Asao General Hospital, Kawasaki, Japan (K.N.); Department of Cardiology, Tokyo Metropolitan Hiroo Hospital, Tokyo, Japan (H.S.); and Department of Molecular Pathophysiology, Nagasaki University Graduate School of Biomedical Sciences, Nagasaki, Japan (N.M.).

The online-only Data Supplement is available at http://circep.ahajournals.org/lookup/suppl/doi:10.1161/CIRCEP.111.969972/-/DC1.

*These authors shared first authorship.

Correspondence to Akinori Kimura, MD, PhD, Department of Molecular Pathogenesis, Medical Research Institute, Tokyo Medical and Dental University, 1-5-45 Yushima, Bunkyo-ku, Tokyo 113–8510, Japan (e-mail akitis@tmd.ac.j); or Naomasa Makita, MD, PhD, Department of Molecular Pathophysiology, Nagasaki University Graduate School of Biomedical Sciences, 1-12-4 Sakamoto, Nagasaki 852-8523, Japan (e-mail: makitan@nagasaki-u.ac.jp).

proteins regulating sodium channel function, such as glycerol-3-phosphate dehydrogenase-1–like enzyme and small subunits of sodium channel (hNavβ1 and hNavβ3) also are associated with BrS and the loss of hNav1.5 function.[16–18]

Excitation–contraction coupling is indispensable for the excitation of cardiomyocytes and is regulated by the functional association of T-tubules and sarcoplasmic reticulum.[19] It has been reported that abnormalities of T-tubules or sarcoplasmic reticulum can cause ventricular arrhythmias.[20–22] One of the components of T-tubules and sarcoplasmic reticulum is sarcolemmal membrane–associated protein (SLMAP), of which the gene *SLMAP* maps to chromosome 3p14.3–21.2 and encodes several isoforms of SLMAP via alternative splicing.[23] SLMAP is composed of several functional domains, including a forkhead-associated domain, a RecN domain, 2 leucine zipper domains, and a tail-anchor domain that is expressed as a mutually exclusive TM1 or TM2 domain. The tail-anchor domains play a pivotal role in subcellular targeting of SLMAP.[24] It is known that a ubiquitously expressed isoform, SLMAP3, is encoded by an open reading frame from the start codon in exon 1, whereas the other isoforms, SLMAP1 and SLMAP2, expressed abundantly in striated muscles including heart, are encoded by the other overlapping reading frames from different start codons.[25] Although the functional involvement of SLMAP in cardiac pathophysiology is largely unknown, SLMAP is a candidate gene to search for mutations in arrhythmias including BrS of unknownetiology.

In this study, we analyzed BrS patients for *SLMAP* mutations and investigated the functional significance of the identified mutations. The disease-associated *SLMAP* mutations decreased the cell surface expression of hNav1.5 and reduced the I_{Na} in transfected cells. This is the first report demonstrating the functional association of SLMAP with hNav1.5 and a novel pathogenic substrate for BrS.

Materials and Methods

Subjects

We studied 190 genetically unrelated patients with BrS. All patients manifested with a BrS diagnostic ECG pattern and were all free from mutations in *SCN5A* (BrS1).[26] Control subjects were 94 to 380 ethnic-matched healthy individuals. Blood sample was obtained from each subject after an informed consent for gene analysis was given. Data from public available databases as the 1000 genome project (http://www.1000genomes.org/) also were analyzed as controls. The research protocol was approved by the Ethics Review Committee of Medical Research Institute, Tokyo Medical and Dental University, the Mayo Foundation Institutional Review Board, and the Medical Ethical Committee of Fondazione IRCCS Policlinico San Matteo.

Mutational Analysis of SLMAP in BrS

Genomic DNA extracted from peripheral blood leukocytes of each individual was subjected to polymerase chain reaction using primer pairs for *SLMAP* (online-only Data Supplement Table I). Polymerase chain reaction products from Japanese patients were analyzed by direct sequencing method, whereas those from white patients underwent denaturing high-performance liquid chromatography and direct sequencing.[27] The sequencing of polymerase chain reaction products was performed using Big Dye Terminator version 3.1 (Applied Biosystems) and ABI3100 DNA analyzer (Applied Biosystems). The patients carrying rare nonsynonymous variations also were analyzed for mutations in all known BrS susceptibility genes (online-only Data Supplement Table II).

Constructs for SLMAP, hNavβ1, and hNav1.5

We obtained cDNA fragments for human SLMAP by reverse-transcription polymerase chain reaction from human heart cDNA. Wild-type (WT) cDNA fragment for SLMAP with TM1 or TM2 domain were amplified, and equivalent cDNA fragments containing a G-to-A substitution in codon 269 (for V269I), a C-to-A substitution in codon 288 (for H288Y), or an A-to-C substitution at codon 710 (for E710A) were created by the primer-mediated mutagenesis method (online-only Data Supplement Table III). The cDNA fragments of SLMAP were cloned into pEGFP-C1 for EGFP-SLMAP, pcDNA3.1 for pcDNA3.1-SLMAP, and pIRES-CD8 for pIRES-CD8-SLMAP. A cDNA fragment of hNavβ1 was cloned into pcDNA3.1-myc, and into His-B to obtain myc, His-hNavβ1. The cDNA fragment of human *SCN5A* was a gift from Dr A.L. George (Vanderbilt University, Nashville, TN). A Flag-tagged hNav1.5 was constructed by inserting a Flag epitope (DYKDDDDK) into the extracellular linker 1 between S1 and S2 in D1 domain after the position of aa154 in the hNav1.5 construct (L1-Flag-hNav1.5).[28] All constructs were sequenced to ensure that no errors were introduced.

Immunofluorescence Microscopy

HEK293 or H9c2 cells were seeded onto culture slides (BD Biosciences); 24 hours later, L1-Flag-hNav1.5 plus each EGFP-SLMAP with or without pcDNA3.1-SLMAP were transfected. After 48 hours of the transfection, the cells were permeabilized and incubated with the primary rabbit anti-Flag polyclonal Ab (Sigma) and secondary Alexa fluor 568 goat anti-rabbit IgG (Molecular Probes). Images of cells were collected and analyzed with LSM510 laser-scanning microscope. To quantify membrane expression of hNav1.5, fluorescence intensity at the entire cell area and the plasma membrane region (2 μm) in the middle *xy* images of *z* series stack were measured, and the ratios of peripheral to total cell area fluorescence intensity (PTAFI) were calculated as described previously.[16] Analyses of labeled cells were performed using ImageJ software (National Institutes of Health).[29]

Silencing of Transfected SLMAP by Small Interfering RNA

Predesigned small interfering RNA (siRNA) for human SLMAP (siRNA ID: s15435) and nonsilencing siRNA as a negative control were purchased from Ambion. HEK293 cells were seeded onto poly-D-Lysine–coated dishes or slides. After 24 hours, the cells were cotransfected with the combination of EGFP-SLMAP and L1-Flag-hNav1.5 with the predesigned siRNA or nonsilencing siRNA. After 48 hours of the transfection, the cells were lysed and subjected to Western blot analyses.

Electrophysiological Studies

We used the tsA-201 cell line, a derivative of HEK293 cell line, in our electrophysiological study, as described previously.[28] In brief, the cells were transfected transiently with either WT or mutant EGFP-SLMAP or pIRES-CD8-SLMAP in combination with pcDNA3.1-Nav1.5. Sodium currents were recorded from the cells that were positive for EGFP or labeled with CD8-Dynabeads using the whole-cell patch-clamp techniques.

Statistical Analysis

Numerical data were expressed as means±SEM. The normal distributions and equal variances of the data in this study were confirmed by using Shapiro-Wilk test or *F* test, respectively. Statistical differences were analyzed using 1-way ANOVA followed by Dunnett test and Student *t* test. $P<0.05$ was considered to be statistically significant.

Table 1. Sequence Variations in Exons of SLMAP Found in Brugada Syndrome Patients and Controls

	Location in Exon	Position at Codon*	Nucleotide Change (Corresponding Amino Acid)	Asian BrS Patients† (n=88)	Japanese Controls (n=94–380)	White BrS Patients (n=102)	dbSNP
1	Exon 1	24	CTG (Leu) to CTA (Leu)	0	0 in 187	1	
2	Exon 1	31	GGC (Gly) to GGT (Gly)	1	3 in 187	0	
3	Exon 2	68	TAT (Tyr) to TTT (Phe)	6	3 in 174	0	
4	Exon 6	193	CTA (Leu) to CTG (Leu)	1	8 in 362	0	
5	Exon 7	217	TTA (Leu) to TTG (Leu)	3	4 in 269	0	rs74857771
6	Exon 8	269	GTT (Val) to ATT (Ile)	1	0 in 380	0	
7	Exon 9	288	CAT (His) to TAT (Tyr)	1	1 in 380	0	
8	Exon 14	408	GGG (Gly) to GGT (Gly)	1	3 in 180	0	
9	Exon 16	447	GAC (Asp) to GAT (Asp)	52	55 in 94	0	rs17058639
10	Exon 19	622	CTT (Leu) to CTA (Leu)	0	0 in 192	4	rs35219531
11	Exon 19	630	CAG (Gln) to CGG (Arg)	0	0 in 192	1	rs35029175
12	Exon 21	681	CAG (Gln) to CAA (Gln)	0	1 in 380	11	rs17745469
13	Exon 21	710	GAA (Glu) to GCA (Ala)	1	0 in 380	0	

BrS indicates Brugada syndrome; and SLMAP, sarcolemmal membrane–associated protein.
*Codon number is that for SLMAP3.
†Japanese patients (n=85) and Korean patients (n=3).

Results

Mutational Analysis of SLMAP

We analyzed 190 BrS patients for mutations in *SLMAP*, and 8 synonymous and 5 nonsynonymous genetic variants were detected (Table 1 and Figure 1A). Among them, 5 variants had been registered in a public database of polymorphisms the single nucleotide polymorphism database (dbSNP) database; Table 1). A nonsynonymous variant p.Tyr68Phe (c.203A>T) was a polymorphism found in both patients and controls at similar frequencies in the Japanese population. The other 4 synonymous variants were rare but may not be disease-causing mutations, because no functional impact was deduced.

Three other variants were identified in the heterozygous state in each patient, p.Val269Ile (c.805G>A), p.His288Tyr (c.862C>T), and p.Glu710Ala (c.2129A>C) (online-only Data Supplement Figure IA and Table 1). The p.Val269Ile and p.Glu710Ala missense mutations (V269I and E710A, respectively) were found in a 46-year-old male patient and in a 57-year-old male patient, respectively, who both experienced syncope and showed spontaneous saddle-back (V269I) or coved-type (E710A) ST elevation on ECG, whereas the p.His288Tyr variant (H288Y) was found in a 51-year-old male patient who had development of a diagnostic BrS pattern only after the infusion of class Ic drugs. ECG records of the patients with V269I or E710A showed no apparent conduction delay (Figure 1B and 1C, online-only Data Supplement Table IV). In addition, both of them did not show obvious cardiac structural and functional abnormalities. All these substitutions were predicted to affect evolutionary conserved residues of SLMAP (online-only Data Supplement Figure IB). Both V269I and H288Y should be expressed only in SLMAP3, whereas E710A would be expressed in all SLMAP isoforms (Figure 1A). Because these variants were found in Japanese patients, we analyzed 380 Japanese individuals selected at random. V269I and E710A were not detected in the controls, whereas H288Y was observed in 1 control (Table 1). In addition, V269I and E710A were absent among the 1094 individuals, descendants of various ancestries (381 European ancestry, 246 West African ancestry, 181 American ancestry, and 286 East Asian ancestry), whereas H288Y was reported in the 1000 genome project. The patients carrying these variants had no mutation in all the known BrS susceptibility genes and no family history of arrhythmia or sudden cardiac death. Family studies were not performed.

Decreased Cell Surface Expression of hNav1.5 in the Presence of Mutant SLMAPs

Because the majority of BrS-associated mutations are known to affect the hNav1.5 properties, including loss of cell surface expression, we tested whether the SLMAP mutations would affect the subcellular localization of hNav1.5. We examined expression of SLMAPs in cell lines available for transfection experiments and found the endogenous expression in HEK293, tsA-201, and H9c2 cells (online-only Data Supplement Figure II). We then analyzed the cell surface expression of hNav1.5 in HEK293 cells cotransfected with L1-Flag-hNav1.5 and EGFP-SLMAP3 or EGFP-SLMAP1 with the TM1 or TM2 domain (Figure 2). The PTAFI ratio of hNav1.5 in the cotransfected cells of L1-Flag-hNav1.5 and EGFP-SLMAP3-TM1-WT was similar to the PTAFI ratio in the transfectants of L1-Flag-hNav1.5 and EGFP-SLMAP3-TM2-WT. However, the PTAFI ratios in the transfected cells of L1-Flag-hNav1.5 with EGFP-SLMAP3-TM1-V269I, EGFP-SLMAP3-TM2-V269I, EGFP-SLMAP3-TM1-E710A, or EGFP-SLMAP3-TM2-E710A were significantly decreased, whereas the PTAFI ratios in the transfectants of L1-Flag-hNav1.5 with EGFP-SLMAP3-TM1-H288Y or EGFP-SLMAP3-TM2-H288Y were not significantly altered (Figure 2, online-only Data Supplement Table V). E710A in SLMAP3 also should be expressed as E261A in SLMAP1, and we found that the PTAFI ratios in the L1-Flag-hNav1.5 transfected cells of either EGFP-SLMAP1-TM1-E261A or EGFP-SLMAP1-TM2-E261A were significantly decreased.

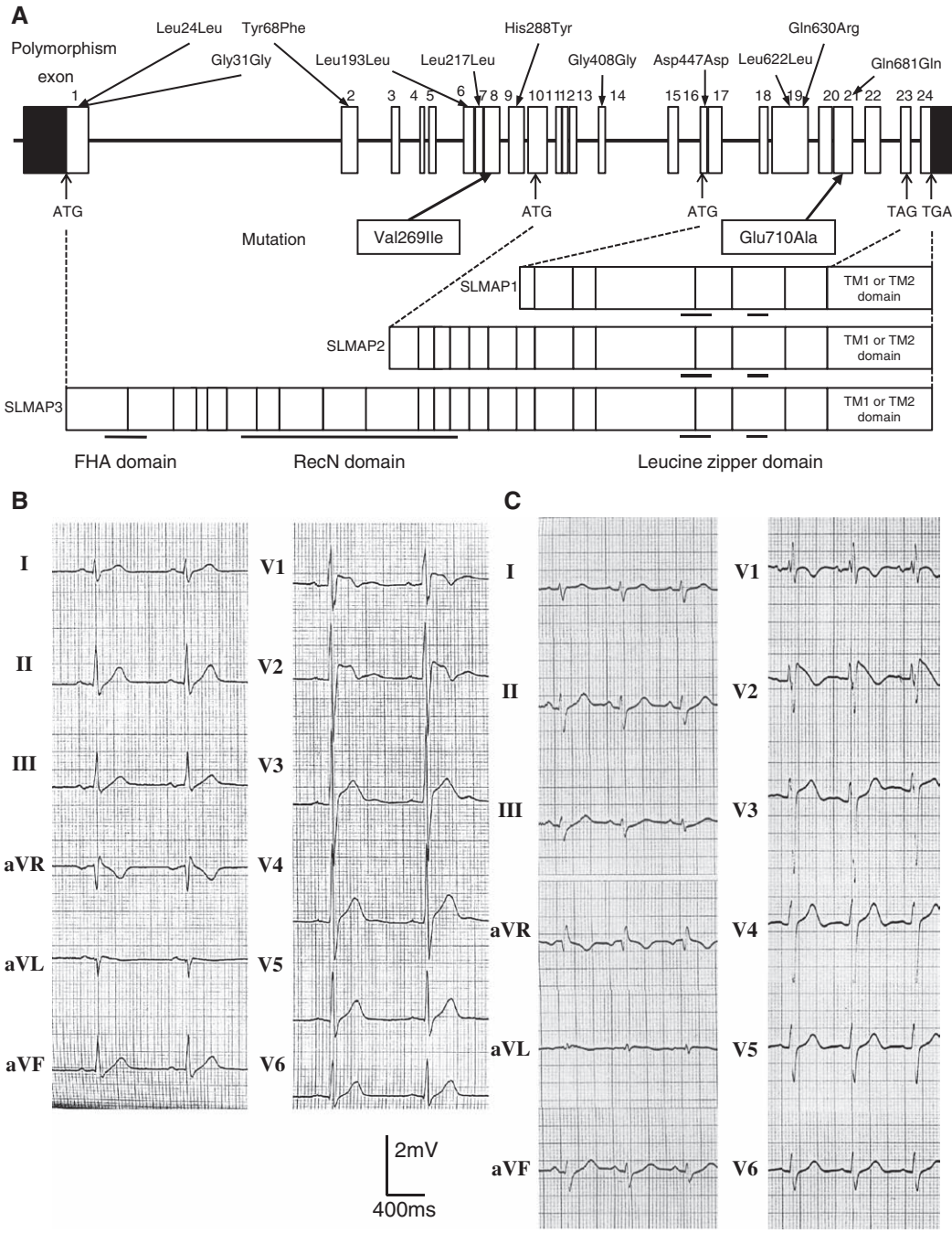

Figure 1. Mutational analysis of *SLMAP* gene in Brugada syndrome (BrS)**. A**, Structure of *SLMAP* and sequence variations found in this study. **B** and **C**, Representative ECG records of the patients carrying V269I (**B**) or E710A (**C**). Both of them showed no apparent cardiac conduction delay.

To mimic a heterozygous state of *SLMAP* mutations, HEK293 cells were cotransfected with L1-Flag-hNav1.5, SLMAP3-TM1-WT, and each mutant SLMAP construct (Figure 3, online-only Data Supplement Table V). The PTAFI ratios in the L1-Flag-hNav1.5–transfected cells with both WT and mutant SLMAP were similar to those in the L1-Flag-hNav1.5–transfected cells with each mutant SLMAP, suggesting that V269I and E710A reduced the surface expression of hNav1.5 by a dominant-negative mechanism.

We also investigated the reduction of hNav1.5 expression by the *SLMAP* mutations in a rat cardiomyocyte–derived cell line, H9c2. H9c2 cells were transiently transfected with L1-Flag-hNav1.5 and either WT or mutant EGFP-SLMAP3-TM1. It was found that V269I and E710A mutations, but not H288Y, diminished the surface expression of hNav1.5 (online-only Data Supplement Figure III).

Silencing of Mutant SLMAPs Rescued the Cell Surface Expression of hNav1.5

To demonstrate the effect of *SLMAP* mutations on the surface expression of hNav1.5 by another method, we investigated whether silencing of the SLMAP mutants could rescue the decreased surface expression of hNav1.5. Silencing efficacy of predesigned siRNA for human *SLMAP* was evaluated, and it was

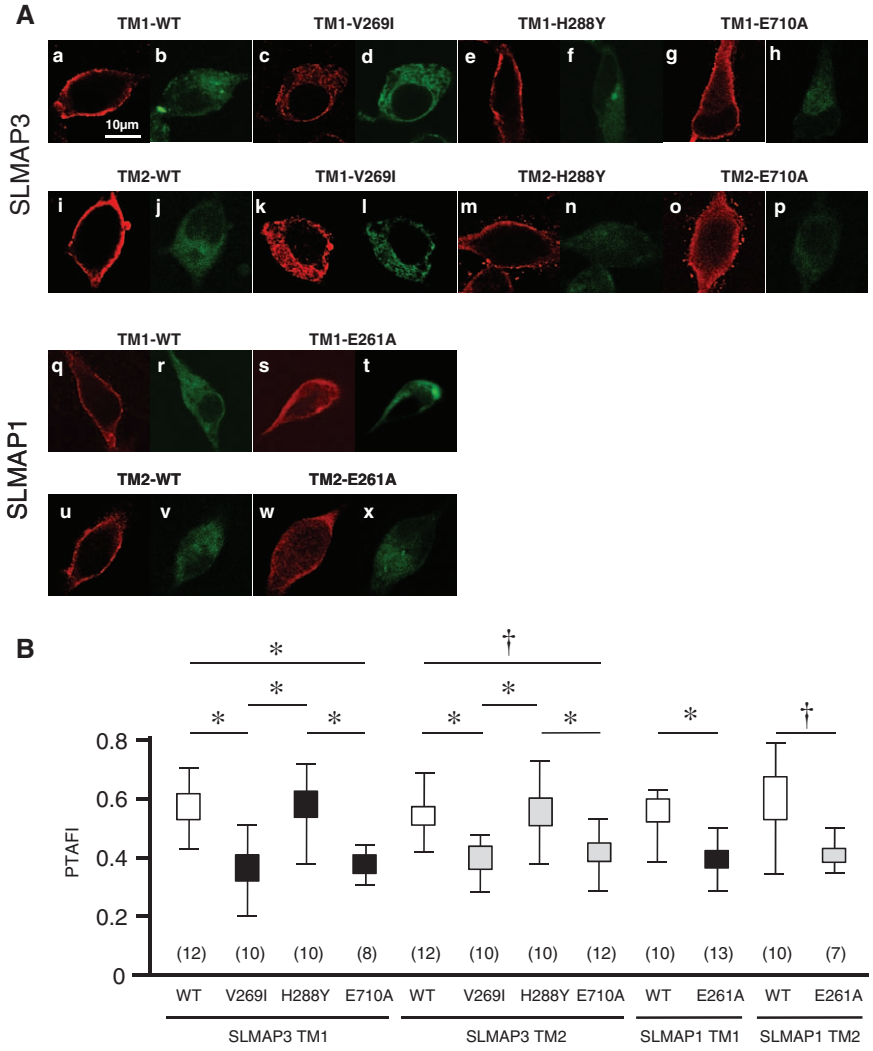

Figure 2. Fluorescence images of transiently expressed EGFP sarcolemmal membrane–associated protein (SLMAP) in HEK293 cells**. A**, Representative images of HEK293 cells cotransfected with L1-Flag-hNav1.5 and EGFP-SLMAP3-TM1-WT (**a** and **b**), EGFP-SLMAP3-TM1-V269I (**c** and **d**), EGFP-SLMAP3-TM1-H288Y (**e** and **f**), EGFP-SLMAP3-TM1-E710A (**g** and **h**), EGFP-SLMAP3-TM2-WT (**i** and **j**), EGFP-SLMAP3-TM2-V269I (**k** and **l**), EGFP-SLMAP3-TM2-H288Y (**m** and **n**), EGFP-SLMAP3-TM2-E710A (**o** and **p**), EGFP-SLMAP1-TM1-WT (**q** and **r**), EGFP-SLMAP1-TM1-E261A (**s** and **t**), EGFP-SLMAP1-TM2-WT (**u** and **v**), or EGFP-SLMAP1-TM2-E261A (**w** and **x**). The cells were permeabilized and stained with anti-Flag Ab (red; **a**, **c**, **e**, **g**, **i**, **k**, **m**, **o**, **q**, **s**, **u**, and **w**). Expression of EGFP-SLMAP is shown in **b**, **d**, **f**, **h**, **j**, **l**, **n**, **p**, **r**, **t**, **v**, and **x** (green). Scale bar, 10 μm. **B**, The ratio of peripheral to total cell area fluorescence intensity (PTAFI) of expressed L1-Flag-hNav1.5 in the transfected cells. Numbers of the analyzed cells are indicated at the bottom of each bar. **P*<0.001; †*P*<0.01.

found that administration of siRNA at a final concentration of 30 nmol/L completely inhibited the SLMAP expression (Figure 4). HEK293 cells were transfected with the combinations of L1-Flag-hNav1.5, each EGFP-SLMAP construct, and predesigned siRNA to analyze the localization of hNav1.5.

The PTAFI ratios in the transfected cells of L1-Flag-hNav1.5 with each EGFP-SLMAP3 or EGFP-SLMAP1 were not changed in the presence of nonsilencing siRNA (Figure 4A). The PTAFI ratios in the cells expressing L1-Flag-hNav1.5 with EGFP-SLMAP3 of either WT or H288Y with the TM1 or TM2 domain were not significantly different between the presence of predesigned siRNA and nonsilencing siRNA (Figure 4B, online-only Data Supplement Table VI). However, the PTAFI ratios in the cells expressing L1-Flag-hNav1.5 with EGFP-SLMAP3-TM1-V269I or EGFP-SLMAP3-TM2-V269I were significantly higher in the presence of predesigned siRNA than in the presence of nonsilencing siRNA. Similarly, the ratios in the transfectants of L1-Flag-hNav1.5 with EGFP-SLMAP3-TM1-E710A or EGFP-SLMAP3-TM2-E710A were significantly higher in the presence of predesigned siRNA than in the presence of nonsilencing siRNA. The predesigned siRNA also could suppress the impaired surface expression of hNav1.5 caused by the E261A mutation in SLMAP1 (online-only Data Supplement Figure V and online-only Data Supplement Table V). The rescued expression levels, however, were similar to those in the L1-Flag-hNav1.5 transfected cells of EGFP-SLMAP1-WT with either predesigned siRNA or nonsilencing siRNA. These data indicated that the decreased surface expression of hNav1.5 was caused by the *SLMAP* mutations.

Altered Electrophysiological Characters Caused by the SLMAP Mutations

Because the impaired intracellular trafficking of hNav1.5 should result in the reduced hNav1.5 function, we investigated potential effects of the SLMAP mutants on the hNav1.5 kinetics. Whole-cell patch-clamp recordings were obtained from tsA-201 cells transiently transfected with pcDNA3.1-hNav1.5 in combination with EGFP-SLMAP3-WT or EGFP-SLMAP1-WT carrying either TM1 or TM2 domain. Peak current density of I_{Na} (pA/pF) recorded from the cells cotransfected with pcDNA3.1-hNav1.5 and EGFP-C1 was used as a control (Figure 5 and online-only Data Supplement Figures V and VI). It was found that the peak current densities recorded from the

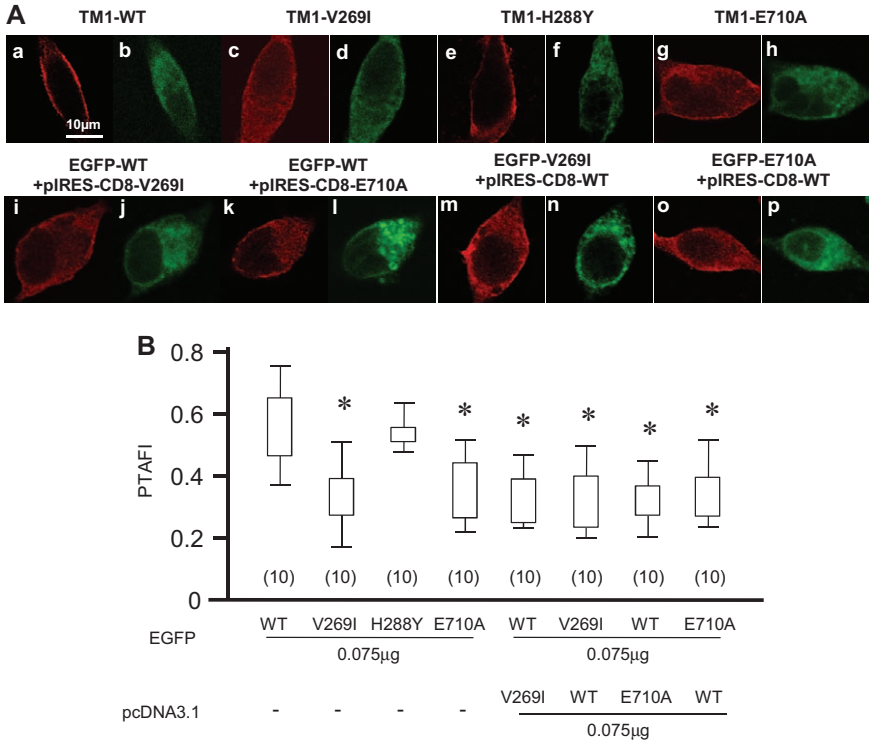

Figure 3. Fluorescence images of transiently expressed EGFP sarcolemmal membrane–associated protein (SLMAP) and pcDNA3.1-SLMAP in HEK293 cells. **A**, Representative images of HEK293 cells cotransfected with L1-Flag-hNav1.5 and EGFP-SLMAP3-TM1-WT (**a** and **b**), EGFP-V269I (**c** and **d**), EGFP-H288Y (**e** and **f**), EGFP-E710A (**g** and **h**), EGFP-WT plus pcDNA3.1-V269I (**i** and **j**), EGFP-V269I plus pcDNA3.1-WT (**k** and **l**), EGFP-WT plus pcDNA3.1-E710A (**m** and **n**), or EGFP-E710A plus pcDNA3.1-WT (**o** and **p**), The cells were permeabilized and stained with anti-Flag Ab (red; **a**, **c**, **e**, **g**, **i, k**, **m**, and **o**). Expression of EGFP-SLMAP is shown in **b**, **d**, **f**, **h**, **j**, **l**, **n**, and **p** (green). Scale bar, 10 μm. **B**, The ratio of peripheral to total cell area fluorescence intensity (PTAFI) of expressed L1-Flag-hNav1.5 in the transfected cells. Numbers of the analyzed cells are indicated at the bottom of each bar. *P<0.001.

transfected cells of pcDNA3.1-hNav1.5 with EGFP-SLMAP3 or EGFP-SLMAP1 in the TM1 or TM2 domain were not significantly different from that of the control. In addition, they did not show any significant changes in the activation and inactivation kinetics of I_{Na} and the time course of recovery from inactivation, as compared with EGFP only (Tables 2 and 3).

When we analyzed the effect of mutant SLMAP3 carrying V269I, H288Y, or E710A on the kinetics of hNav1.5 in the transfected cells (Figure 5, online-only Data Supplement Figure V), the peak current densities recorded from the cells cotransfected with pcDNA3.1-hNav1.5 and EGFP-SLMAP3-H288Y were similar to those recorded from the cells cotransfected with pcDNA3.1-hNav1.5 and EGFP-SLMAP3-WT. In clear contrast, the peak current densities of I_{Na} recorded from the cells cotransfected with pcDNA3.1-hNav1.5 and EGFP-SLMAP3-V269I with TM1 or TM2 domain were significantly smaller than those recorded from the cells cotransfected with pcDNA3.1-hNav1.5 and EGFP-SLMAP3-WT with the TM1 or TM2 domain by 56.5% and 51.9%, respectively (Tables 2 and 3). In addition, the peak current densities recorded from the cells cotransfected with pcDNA3.1-hNav1.5 and EGFP-SLMAP3-E710A with the TM1 or TM2 domain were significantly smaller than those recorded from the cells cotransfected with pcDNA3.1-hNav1.5 and EGFP-SLMAP3-WT with the TM1 or TM2 domain by 49.7% and 40.7%, respectively. However, none of the EGFP-SLMAP3-V269I, EGFP-SLMAP3-H288Y, and EGFP-SLMAP3-E710A caused significant changes in the activation and inactivation kinetics of I_{Na} and the time constants for recovery from inactivation.

We also investigated whether E261A mutation in SLMAP1 would show an effect on hNav1.5 kinetics as E710A mutation in SLMAP3 did. It was demonstrated that the peak current densities recorded from the cells cotransfected with pcDNA3.1-hNav1.5 and EGFP-SLMAP1-E261A were significantly lower than those recorded from the cells cotransfected with pcDNA3.1-hNav1.5 and EGFP-SLMAP1-WT by ≈40% without any significant changes in the activation and inactivation kinetics of I_{Na} and the time constants for recovery from inactivation (Tables 2 and 3, online-only Data Supplement Figure VI).

To exclude a possibility that the EGFP fused to SLMAP might affect the function of SLMAP or hNav1.5, we recorded I_{Na} from cells transiently transfected with pcDNA3.1-hNav1.5 and pIRES-CD8-SLMAP3 with or without mutation or variation (online-only Data Supplement Figure VII, online-only Data Supplement Table VII). It was observed that pIRES-CD8-SLMAP3-V269I and pIRES-CD8-SLMAP3-E710A decreased the peak current densities of I_{Na} to a similar extent as EGFP-fused SLMAPs. The effect of SLMAP mutations appeared to be exerted by a dominant-negative mechanism, as observed for the trafficking impairment.

Binding Between SLMAP and hNav1.5

Because the *SLMAP* mutations might modulate I_{Na} through a physical interaction with hNav1.5, we investigated whether SLMAP bound hNav1.5. No direct interaction between SLMAP and hNav1.5 was found under the condition in which the binding of hNav1.5 and hNavβ1 could be detected (online-only Data Supplement Figure VIII).

Discussion

Arrhythmias can be caused by mutations in the genes encoding ion channels producing action potentials.[30] In BrS, sodium current is more frequently affected than the other currents, such as calcium and potassium currents.[31] The affected sodium current is caused by mutations in the gene encoding hNav1.5, *SCN5A*, or genes for modifier proteins.[13,16–18] Prevalence of *SCN5A* mutations in BrS is ≈20%, whereas the prevalence of

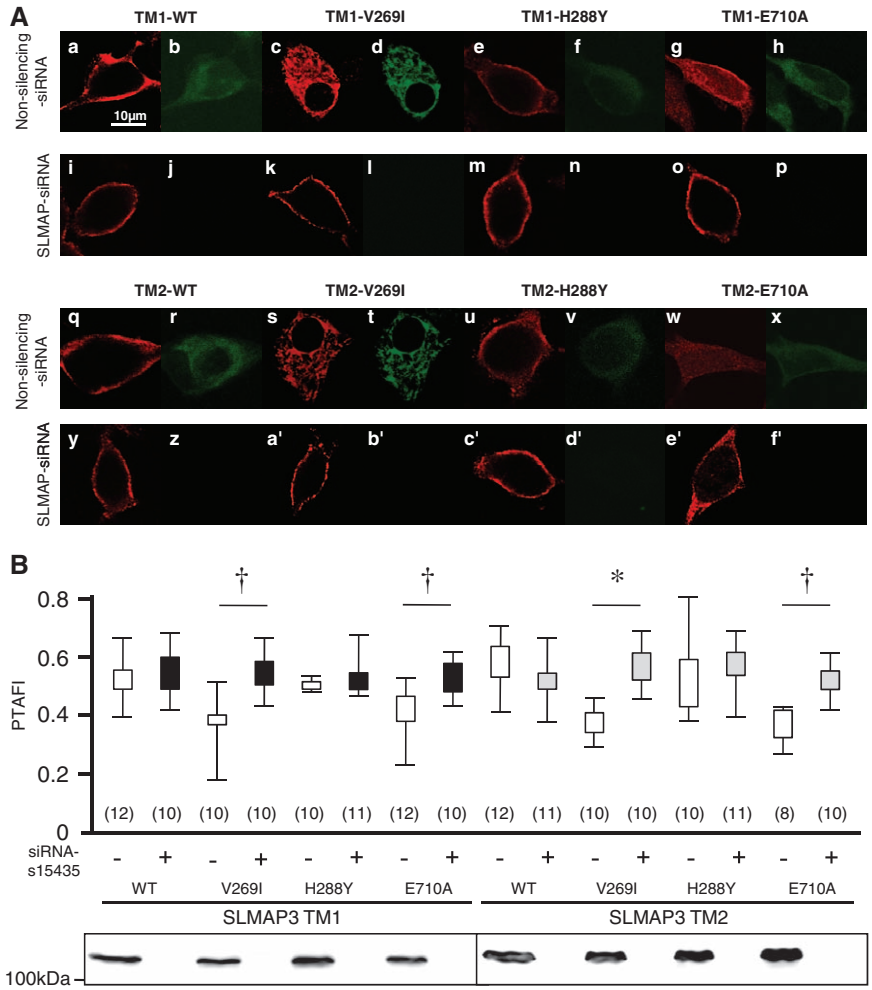

Figure 4. Silencing of transiently expressed *SLMAP3* in HEK293 cells**. A**, Representative images of HEK293 cells cotransfected with L1-Flag-hNav1.5 and EGFP sarcolemmal membrane–associated protein (SLMAP) 3-TM1-WT (**a**, **b**, **i** and **j**), EGFP-SLMAP3-TM1-V269I (**c**, **d**, **k**, and **l**), EGFP-SLMAP3-TM1-H288Y (**e**, **f**, **m** and **n**), EGFP-SLMAP3-TM1-E710A (**g**, **h**, **o**, and **p**), EGFP-SLMAP3-TM2-WT (**q**, **r**, **y**, and **z**), EGFP-SLMAP3-TM2-V269I (**s**, **t**, **a′**, and **b′**), EGFP-SLMAP3-TM2-H288Y (**u**, **v**, **c′**, and **d′**), or EGFP-SLMAP3-TM2-E710A (**w**, **x**, **e′**, and **f′**) in the presence of nonsilencing (**a–h** and **q–x**) or predesigned (**i–p** and **y–f′**) small interfering RNA (siRNA). The cells were permeabilized and stained with anti-Flag Ab (red; **a**, **c**, **e**, **g**, **i**, **k**, **m**, **o**, **q**, **s**, **u**, **w**, **y**, **a′**, **c′,** and **e′**). Expression of EGFP-SLMAP3 is shown in **b**, **d**, **f**, **h**, **j**, **l**, **n**, **p**, **r**, **t**, **v**, **x**, **z**, **b′**, **d′**, and **f′** (green). Scale bar, 10 μm. **B**, The ratio of peripheral to total cell area fluorescence intensity (PTAFI) of expressed L1-Flag-hNav1.5 in the transfected cells. Numbers of analyzed cells are indicated at the bottom of each bar. Silencing of EGFP-SLMAP3 by predesigned siRNA against human SLMAP (s15435) is shown in the **bottom**. PTAFIs were compared between the cells transfected with nonsilencing siRNA and with SLMAP-siRNA. **P*<0.001; †*P*<0.01; ‡*P*<0.05.

mutations in the other genes is relatively low.[31–34] In the present study, genetic analysis of *SLMAP* revealed a low prevalence of mutation, 2 in 190 BrS patients. Functional studies of the mutations suggested that SLMAP might be a modifier protein of hNav1.5 function. Because hNav1.5 and modifier proteins compose the sodium channel complex to generate and regulate the sodium current, functional abnormality of any components of the complex might alter the electrophysiological characters of cardiomyocytes.[30]

BrS-associated mutations in genes for the components of sodium channel complex usually result in loss of hNav1.5 function, including the voltage-dependent shift in the steady-state inactivation and activation profile, increased onset of inactivation, and decreased I_{Na}.[14] It was reported that mutations in the gene for hNavβ1, an auxiliary subunit of the sodium channel, affected the modulation of hNav1.5 channel gating.[17] Here, we demonstrate that the *SLMAP* mutations do not affect the voltage dependence in inactivation or activation profiles, suggesting that the mutations do not biophysically alter the hNav1.5 channel gating. However, the *SLMAP* mutations exerted a biogenic effect by reducing the surface expression of hNav1.5,

Table 2. Electrophysiological Properties of Transfected tsA-201 Cells of pcDNA3.1-hNav1.5 and Sarcolemmal Membrane–Associated Protein Constructs With Sarcolemmal Membrane–Associated Protein 3 Constructs

	WT-TM1	n	V269I-TM1	n	H288Y-TM1	n	E710A-TM1	n	WT-TM2	n	V269I-TM2	n	H288Y-TM2	n	E710A-TM2	n
Current density at −30 mV (pA/pF)	−336.2±63.6	11	−146.3±10.7*	9	−310.3±63.7	7	−169.2±15.7*	16	−373.2±45.9	13	−179.5±26.1*	11	−283.2±55.7	12	−221.4±40.6*	13
Voltage dependence of inactivation ($V_{1/2}$, mV)	−84.72±1.26	12	−86.13±0.98	9	−84.28±1.54	7	−84.47±1.15	15	−86.31±0.94	15	−86.32±0.79	13	−83.4±1.15	15	−85.36±1.37	15
Voltage dependence of activation ($V_{1/2}$, mV)	−46.40±1.85	8	−44.62±1.00	9	−47.46±1.72	7	−43.68±1.09	20	−47.07±1.25	13	−47.23±1.17	9	−45.51±1.59	12	−44.11±1.34	12
Time required for e^{-1} fraction recovery, ms	8.39±1.16	9	9.34±1.28	9	9.88±1.21	7	9.40±1.29	17	9.31±1.11	11	9.11±1.00	9	9.42±2.11	12	9.40±1.29	14

WT indicates wild-type.
**P*<0.05 vs WT.

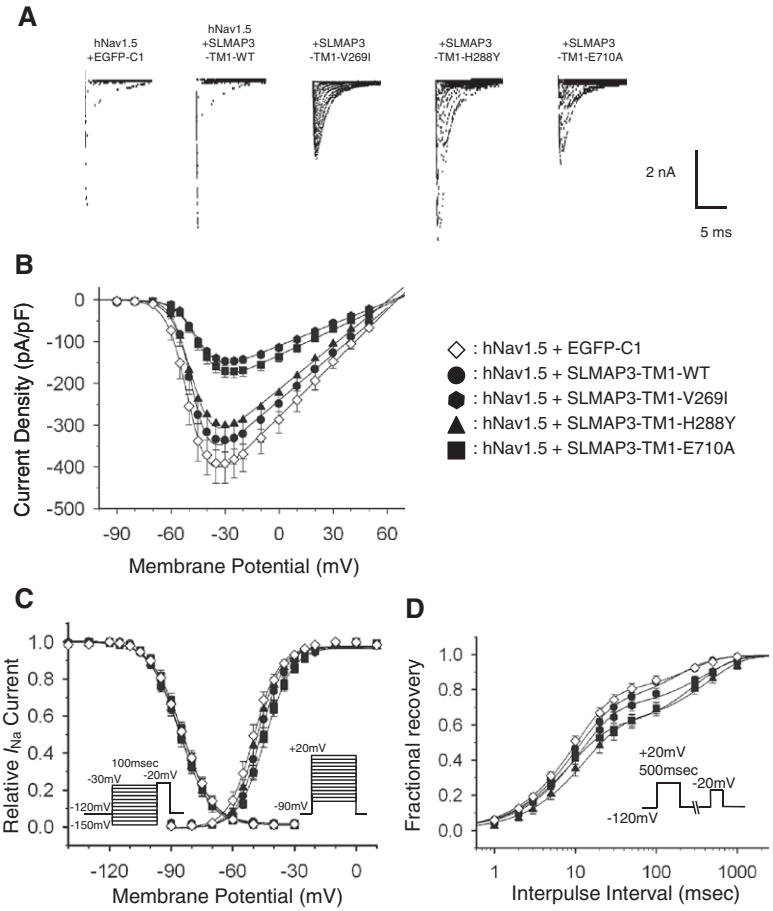

Figure 5. Sodium currents recorded from tsA-201 cells cotransfected with Nav1.5 and sarcolemmal membrane–associated protein (SLMAP) 3-TM1 constructs**. A**, Representative sodium currents were recorded from transfected tsA-201 cells of pcDNA3.1-hNav1.5 with EGFP, EGFP-SLMAP3-wild type (WT), EGFP-SLMAP3-V269I, EGFP-SLMAP3-H288Y, or EGFP-SLMAP3-E710A with TM1 domain. These traces were recorded with the whole-cell configuration as shown in the inset. **B**, Current–voltage relationship for peak I_{Na}. EGFP-SLMAP3-V269I and EGFP-SLMAP3-E710A showed a significant decline of peak current densities by 56.5% and 49.7% (n=11 for WT, n=9 for V269I, n=16 for E710A) at –30mV, whereas EGFP-SLMAP3-H288Y (n=7) did not alter the peak current density. **C**, The voltage dependence of steady-state fast inactivation and activation recorded from the transfected cells of pcDNA3.1-hNav1.5 in combination with EGFP, EGFP-SLMAP3-V269I, SLMAP3-H288Y, or EGFP-SLMAP3-E710A with TM1 domain were similar to that from the cells cotransfected with pcDNA3.1-hNav1.5 and EGFP-SLMAP3-WT with TM1 domain. **D**, Recovery from inactivation assessed by the double-pulse protocol was nearly identical among WT, V269I, H288Y, and E710A in SLMAP3. The 2-pulse protocol is shown in the inset.

culminating in decreased peak sodium current density and BrS susceptibility.

SLMAP is a member of tail-anchored proteins, which have a single TM domain at the C-terminal end to determine the subcellular localization. Tail-anchored proteins are involved in a variety of important cellular functions such as apoptosis, protein translocation, and membrane fusion in the organelles, where the proteins are anchored by the TM domain.[35] In the present study, we used SLMAPs carrying either the TM1 or TM2 domain and demonstrated that the mutation-related functional alteration could be observed similarly in any of the SLMAP isoforms with different TM domains, suggesting that the impaired hNav1.5 trafficking was attributable to the functional alterations of SLMAP in the endoplasmic reticulum, where SLMAP with either TM1 or TM2 domain could be localized.[24] Interestingly, SLMAP regulates the translocation of insulin-regulated glucose transporter GLUT4 from an intracellular compartment to the plasma membrane in adipose tissue, demonstrating the role of SLMAP in the intracellular trafficking.[36]

We showed that the SLMAP mutants impaired the surface expression of hNav1.5. However, no direct binding of hNav1.5 and SLMAP was detected in this study, speculating that SLMAP might indirectly contribute to the action potential in cardiomyocytes by modulating hNav1.5 localization. It has been demonstrated that MOG1 binds hNav1.5, and a MOG1 mutation causes BrS via an intracellular trafficking defect.[13] Then, the mechanism of impaired hNav1.5 trafficking caused by the SLMAP mutations was different from that caused by the MOG1 mutation. Recently, it was reported that a Z-disc protein, ZASP, formed a macromolecular

Table 3. Electrophysiological Properties of Transfected tsA-201 Cells of pcDNA3.1-hNav1.5 and Sarcolemmal Membrane–Associated Protein Constructs With Sarcolemmal Membrane–Associated Protein 1 Constructs and No Sarcolemmal Membrane–Associated Protein Control

	WT-TM1	n	E261A-TM1	n	WT-TM2	n	E261A-TM2	n	EGFP-C1	n
Current density at –30mV (pA/pF)	–413.6±52.6	8	–253.4±44.5†	14	–410.2±39.7	11	–246.6±26.7*	13	–394.0±65.8	15
Voltage dependence of inactivation ($V_{1/2}$, mV)	–86.61±1.29	9	–87.46±1.25	15	–80.46±1.19	12	–81.69±0.98	13	–83.25±1.41	15
Voltage dependence of activation ($V_{1/2}$, mV)	–49.29±2.14	8	–43.19±1.60	14	–45.99±1.28	11	–41.39±1.20	13	–49.83±1.99	15
Time required for e^{-1} fraction recovery (msec)	6.75±0.61	15	7.35±0.55	14	8.67±0.67	10	7.93±1.16	12	7.85±0.89	15

WT indicates wild-type.
*P<0.001.
†P<0.05 vs WT.

complex with hNav1.5, but there was no direct interaction between ZASP and hNav1.5, and a *ZASP* mutation disturbed the hNav1.5 function without affecting the localization of hNav1.5.[37] The function of hNav1.5 in cardiomyocytes may be regulated by a fine-tuning mechanism in which many proteins are directly or indirectly involved. Finally, although the loss of hNav1.5 function is often associated with prolongation of PR and QRS, no conduction delay was observed in ECGs from both patients carrying the *SLMAP* mutations. This might be attributable to the difference in severity of functional loss, or it might depend on the nature of affected genes. Further studies will be required to clarify the mechanisms causing the phenotypic difference in functional loss of hNav1.5.

In summary, we identified 2 *SLMAP* missense mutations associated with BrS, and the functional analyses indicated that mutant SLMAP biogenically impaired hNav1.5 trafficking. Like many of the BrS-associated auxiliary proteins, SLMAP-mediated BrS joins the most common pathogenic mechanism of BrS, sodium current loss-of-function BrS.

Sources of Funding

This work was supported in part by a grant-in-aid for Scientific Research from the Ministry of Education, Culture, Sports, Science, and Technology, Japan (22390157, 23132507, and 23659414 to A. Kimura, and 22136007 to N. Makita), Health and Labor Sciences research grant for research on measures of intractable diseases from the Ministry of Health, Labour, and Welfare, Japan (2010–119 to A. Kimura and 2010–145 to N. Makita), grants for Basic Scientific Cooperation Program between Japan and Korea from the Japan Society for the Promotion of Science (A. Kimura), National Research Foundation of Korea Grant (NRF-2010-E00024) (J-E. Park), a research grant from the Association Française contre les Myopathie (T. Arimura), Joint Usage/Research Program of Medical Research Institute Tokyo Medical and Dental University (A. Kimura), and the Windland Smith Rice Comprehensive Sudden Cardiac Death Program at the Mayo Clinic (M.J. Ackerman). This work also was supported by the follow-up grants provided from the Tokyo Medical and Dental University (A. Kimura).

Disclosures

M.J. Ackerman is a consultant for Transgenomic/FAMILION. Intellectual property derived from M.J. Ackerman's research program resulted in license agreements in 2004 between Mayo Clinic Health Solutions (formerly Mayo Medical Ventures) and PGxHealth (recently acquired by Transgenomic). The other authors have no conflicts to report.

References

1. Brugada P, Brugada J. Right bundle branch block, persistent ST segment elevation and sudden cardiac death: a distinct clinical and electrocardiographic syndrome. A multicenter report. *J Am Coll Cardiol*. 1992;20:1391–1396.
2. Chen PS, Priori SG. The Brugada syndrome. *J Am Coll Cardiol*. 2008;51:1176–1180.
3. Hermida JS, Lemoine JL, Aoun FB, Jarry G, Rey JL, Quiret JC. Prevalence of the brugada syndrome in an apparently healthy population. *Am J Cardiol*. 2000;86:91–94.
4. Miyasaka Y, Tsuji H, Yamada K, Tokunaga S, Saito D, Imuro Y, Matsumoto N, Iwasaka T. Prevalence and mortality of the Brugada-type electrocardiogram in one city in Japan. *J Am Coll Cardiol*. 2001;38:771–774.
5. Antzelevitch C, Brugada P, Borggrefe M, Brugada J, Brugada R, Corrado D, Gussak I, LeMarec H, Nademanee K, Perez Riera AR, Shimizu W, Schulze-Bahr E, Tan H, Wilde A. Brugada syndrome: report of the second consensus conference: endorsed by the Heart Rhythm Society and the European Heart Rhythm Association. *Circulation*. 2005;111:659–670.
6. Schulze-Bahr E, Eckardt L, Breithardt G, Seidl K, Wichter T, Wolpert C, Borggrefe M, Haverkamp W. Sodium channel gene (SCN5A) mutations in 44 index patients with Brugada syndrome: different incidences in familial and sporadic disease. *Hum Mutat*. 2003;21:651–652.
7. Kapplinger JD, Tester DJ, Alders M, Benito B, Berthet M, Brugada J, Brugada P, Fressart V, Guerchicoff A, Harris-Kerr C, Kamakura S, Kyndt F, Koopmann TT, Miyamoto Y, Pfeiffer R, Pollevick GD, Probst V, Zumhagen S, Vatta M, Towbin JA, Shimizu W, Schulze-Bahr E, Antzelevitch C, Salisbury BA, Guicheney P, Wilde AA, Brugada R, Schott JJ, Ackerman MJ. An international compendium of mutations in the SCN5A-encoded cardiac sodium channel in patients referred for Brugada syndrome genetic testing. *Heart Rhythm*. 2010;7:33–46.
8. Ueda K, Hirano Y, Higashiuesato Y, Aizawa Y, Hayashi T, Inagaki N, Tana T, Ohya Y, Takishita S, Muratani H, Hiraoka M, Kimura A. Role of HCN4 channel in preventing ventricular arrhythmia. *J Hum Genet*. 2009;54:115–121.
9. Medeiros-Domingo A, Tan BH, Crotti L, Tester DJ, Eckhardt L, Cuoretti A, Kroboth SL, Song C, Zhou Q, Kopp D, Schwartz PJ, Makielski JC, Ackerman MJ. Gain-of-function mutation S422L in the KCNJ8-encoded cardiac K(ATP) channel Kir6.1 as a pathogenic substrate for J-wave syndromes. *Heart Rhythm*. 2010;7:1466–1471.
10. Giudicessi JR, Ye D, Tester DJ, Crotti L, Mugione A, Nesterenko VV, Albertson RM, Antzelevitch C, Schwartz PJ, Ackerman MJ. Transient outward current (I(to)) gain-of-function mutations in the KCND3-encoded Kv4.3 potassium channel and Brugada syndrome. *Heart Rhythm*. 2011;8:1024–1032.
11. Burashnikov E, Pfeiffer R, Barajas-Martinez H, Delpón E, Hu D, Desai M, Borggrefe M, Häissaguerre M, Kanter R, Pollevick GD, Guerchicoff A, Laiño R, Marieb M, Nademanee K, Nam GB, Robles R, Schimpf R, Stapleton DD, Viskin S, Winters S, Wolpert C, Zimmern S, Veltmann C, Antzelevitch C. Mutations in the cardiac L-type calcium channel associated with inherited J-wave syndromes and sudden cardiac death. *Heart Rhythm*. 2010;7:1872–1882.
12. Amin AS, Tan HL, Wilde AA. Cardiac ion channels in health and disease. *Heart Rhythm*. 2010;7:117–126.
13. Kattygnarath D, Maugenre S, Neyroud N, Balse E, Ichai C, Denjoy I, Dilanian G, Martins RP, Fressart V, Berthet M, Schott JJ, Leenhardt A, Probst V, Le Marec H, Hainque B, Coulombe A, Hatem SN, Guicheney P. MOG1: a new susceptibility gene for Brugada syndrome. *Circ Cardiovasc Genet*. 2011;4:261–268.
14. Tfelt-Hansen J, Winkel BG, Grunnet M, Jespersen T. Inherited cardiac diseases caused by mutations in the Nav1.5 sodium channel. *J Cardiovasc Electrophysiol*. 2010;21:107–115.
15. Mohler PJ, Rivolta I, Napolitano C, LeMaillet G, Lambert S, Priori SG, Bennett V. Nav1.5 E1053K mutation causing Brugada syndrome blocks binding to ankyrin-G and expression of Nav1.5 on the surface of cardiomyocytes. *Proc Natl Acad Sci USA*. 2004;101:17533–17538.
16. Hu D, Barajas-Martinez H, Burashnikov E, Springer M, Wu Y, Varro A, Pfeiffer R, Koopmann TT, Cordeiro JM, Guerchicoff A, Pollevick GD, Antzelevitch C. A mutation in the beta 3 subunit of the cardiac sodium channel associated with Brugada ECG phenotype. *Circ Cardiovasc Genet*. 2009;2:270–278.
17. Watanabe H, Koopmann TT, Le Scouarnec S, Yang T, Ingram CR, Schott JJ, Demolombe S, Probst V, Anselme F, Escande D, Wiesfeld AC, Pfeufer A, Kääb S, Wichmann HE, Hasdemir C, Aizawa Y, Wilde AA, Roden DM, Bezzina CR. Sodium channel ß1 subunit mutations associated with Brugada syndrome and cardiac conduction disease in humans. *J Clin Invest*. 2008;118:2260–2268.
18. London B, Michalec M, Mehdi H, Zhu X, Kerchner L, Sanyal S, Viswanathan PC, Pfahnl AE, Shang LL, Madhusudanan M, Baty CJ, Lagana S, Aleong R, Gutmann R, Ackerman MJ, McNamara DM, Weiss R, Dudley SC Jr. Mutation in glycerol-3-phosphate dehydrogenase 1 like gene (GPD1-L) decreases cardiac Na+ current and causes inherited arrhythmias. *Circulation*. 2007;116:2260–2268.
19. Brette F, Orchard C. T-tubule function in mammalian cardiac myocytes. *Circ Res*. 2003;92:1182–1192.
20. Priori SG, Napolitano C, Tiso N, Memmi M, Vignati G, Bloise R, Sorrentino V, Danieli GA. Mutations in the cardiac ryanodine receptor gene (hRyR2) underlie catecholaminergic polymorphic ventricular tachycardia. *Circulation*. 2001;103:196–200.
21. Tiso N, Stephan DA, Nava A, Bagattin A, Devaney JM, Stanchi F, Larderet G, Brahmbhatt B, Brown K, Bauce B, Muriago M, Basso C, Thiene G,

Danieli GA, Rampazzo A. Identification of mutations in the cardiac ryanodine receptor gene in families affected with arrhythmogenic right ventricular cardiomyopathy type 2 (ARVD2). *Hum Mol Genet*. 2001;10:189–194.
22. Lahat H, Pras E, Olender T, Avidan N, Ben-Asher E, Man O, Levy-Nissenbaum E, Khoury A, Lorber A, Goldman B, Lancet D, Eldar M. A missense mutation in a highly conserved region of CASQ2 is associated with autosomal recessive catecholamine-induced polymorphic ventricular tachycardia in Bedouin families from Israel. *Am J Hum Genet*. 2001;69:1378–1384.
23. Guzzo RM, Sevinc S, Salih M, Tuana BS. A novel isoform of sarcolemmal membrane-associated protein (SLMAP) is a component of the microtubule organizing centre. *J Cell Sci*. 2004;117(Pt 11):2271–2281.
24. Byers JT, Guzzo RM, Salih M, Tuana BS. Hydrophobic profiles of the tail anchors in SLMAP dictate subcellular targeting. *BMC Cell Biol*. 2009;10:48.
25. Wigle JT, Demchyshyn L, Pratt MA, Staines WA, Salih M, Tuana BS. Molecular cloning, expression, and chromosomal assignment of sarcolemmal-associated proteins. A family of acidic amphipathic alpha-helical proteins associated with the membrane. *J Biol Chem*. 1997;272:32384–32394.
26. Benito B, Brugada R, Brugada J, Brugada P. Brugada syndrome. *Prog Cardiovasc Dis*. 2008;51:1–22.
27. Ackerman MJ, Tester DJ, Jones GS, Will ML, Burrow CR, Curran ME. Ethnic differences in cardiac potassium channel variants: implications for genetic susceptibility to sudden cardiac death and genetic testing for congenital long QT syndrome. *Mayo Clin Proc*. 2003;78:1479–1487.
28. Makita N, Behr E, Shimizu W, Horie M, Sunami A, Crotti L, Schulze-Bahr E, Fukuhara S, Mochizuki N, Makiyama T, Itoh H, Christiansen M, McKeown P, Miyamoto K, Kamakura S, Tsutsui H, Schwartz PJ, George AL Jr, Roden DM. The E1784K mutation in SCN5A is associated with mixed clinical phenotype of type 3 long QT syndrome. *J Clin Invest*. 2008;118:2219–2229.
29. Abramoff MD, Magelhaes PJ, Ram SJ. Processing with ImageJ. *Biophoton Int*. 2004;11:36–42.
30. Abriel H. Cardiac sodium channel Na(v)1.5 and interacting proteins: Physiology and pathophysiology. *J Mol Cell Cardiol*. 2010;48:2–11.
31. Hedley PL, Jørgensen P, Schlamowitz S, Moolman-Smook J, Kanters JK, Corfield VA, Christiansen M. The genetic basis of Brugada syndrome: a mutation update. *Hum Mutat*. 2009;30:1256–1266.
32. Eckardt L, Probst V, Smits JP, Bahr ES, Wolpert C, Schimpf R, Wichter T, Boisseau P, Heinecke A, Breithardt G, Borggrefe M, LeMarec H, Böcker D, Wilde AA. Long-term prognosis of individuals with right precordial ST-segment-elevation Brugada syndrome. *Circulation*. 2005;111:257–263.
33. Priori SG, Napolitano C, Gasparini M, Pappone C, Della Bella P, Giordano U, Bloise R, Giustetto C, De Nardis R, Grillo M, Ronchetti E, Faggiano G, Nastoli J. Natural history of Brugada syndrome: insights for risk stratification and management. *Circulation*. 2002;105:1342–1347.
34. Crotti L, Kellen CH, Tester D, Castelletti S, Giudessi JR, Torchio M, Medeiros-Domingo A, Savastano S, Will ML, Dagradi F, Schwartz PJ, Ackerman MJ. Spectrum and prevalence of mutations involving BrS1-12-susceptibility genes in a cohort of unrelated patients referred for Brugada syndrome genetic testing: implications for genetic testing. *J Am Col Cardiol*. 2012; 60:1410-1418.
35. Borgese N, Fasana E. Targeting pathways of C-tail-anchored proteins. *Biochim Biophys Acta*. 2011;1808:937–946.
36. Chen X, Ding H. Increased expression of the tail-anchored membrane protein SLMAP in adipose tissue from type 2 Tally Ho diabetic mice. *Exp Diabetes Res*. 2011;2011:421982.
37. Li Z, Ai T, Samani K, Xi Y, Tzeng HP, Xie M, Wu S, Ge S, Taylor MD, Dong JW, Cheng J, Ackerman MJ, Kimura A, Sinagra G, Brunelli L, Faulkner G, Vatta M. A ZASP missense mutation, S196L, leads to cytoskeletal and electrical abnormalities in a mouse model of cardiomyopathy. *Circ Arrhythm Electrophysiol*. 2010;3:646–656.

CLINICAL PERSPECTIVE

Brugada syndrome is an inherited channelopathy characterized by specific ECG findings and sometimes is associated with sudden cardiac arrest. Although the genetic causes of Brugada syndrome in the majority of the patients remain unknown, this disorder has been linked to mutations in the 12 different genes, which cause either a reduction of transient inward sodium or calcium current or an augmentation of transient outward potassium current. In particular, the sodium current is frequently affected because the majority of mutations were found in *SCN5A* encoding a large subunit of cardiac sodium channel hNav1.5. In addition to hNav1.5, auxiliary subunits, hNavβ1 and hNavβ3, and the proteins involved in trafficking, anchoring, or scaffolding of hNav1.5 are involved in propagating sodium current in cardiomyocytes, and mutations in the genes for these components could disturb sodium channel function and result in Brugada syndrome. The underlying molecular mechanisms for the disturbance of sodium channel are abnormalities in gating properties and trafficking efficacy. In this study, we identified the thirteenth disease gene, ie, we revealed that the mutations in *SLMAP* encoding for sarcolemmal membrane–associated protein, a sarcolemmal protein of unknown function, caused Brugada syndrome via a trafficking abnormality of the sodium channel. Our observations deciphered the physiological involvement of sarcolemmal membrane–associated protein in the fine-tuning of electrical propagation in cardiomyocytes and suggest that understanding the trafficking mechanisms of the sodium channel will clarify the pathogenesis of Brugada syndrome to develop a novel therapeutic strategy for Brugada syndrome.

SUPPLEMENTAL MATERIAL

A novel disease gene for Brugada syndrome: sarcolemmal membrane-associated protein gene mutations impair intracellular trafficking of hNav1.5

Ishikawa, Sato, et al. *SLMAP* mutations in Brugada syndrome

Taisuke Ishikawa, DVM,[1 *], Akinori Sato, MD, PhD,[1,2*], Cherisse A. Marcou, BA,[3], David J. Tester, BS,[3], Michael J. Ackerman, MD, PhD,[3], Lia Crotti, MD, PhD,[4-6], Peter J. Schwartz, MD,[5-9], Young Keun On, MD,[10], Jeong-Euy Park, MD,[10], Kazufumi Nakamura, MD, PhD,[11], Masayasu Hiraoka, MD, PhD,[12], Kiyoshi Nakazawa, MD, PhD,[13], Harumizu Sakurada, MD, PhD,[14], Takuro Arimura, DVM, PhD,[1], Naomasa Makita, MD, PhD,[15 #], and Akinori Kimura, MD, PhD,[1 #]

*These authors contributed equally to this work.

[1]Department of Molecular Pathogenesis, Medical Research Institute, Tokyo Medical and Dental University, Tokyo, Japan, [2]Division of Cardiology, Niigata University Graduate School of Medical and Dental Sciences, Niigata, Japan, [3]Departments of Medicine (Division of Cardiovascular Diseases), Pediatrics (Division of Pediatric Cardiology), and Molecular Pharmacology & Experimental Therapeutics, Windland Smith Rice Sudden Death Genomics Laboratory, Mayo Clinic, Rochester, MN, USA, [4]Institute of Human Genetics, Helmholtz Center Munich, Neuherberg, Germany, [5]Department of Molecular Medicine, Section of Cardiology, University of Pavia, Pavia, Italy, [6]Department of Cardiology, Fondazione IRCCS Policlinico S. Matteo, Pavia, Italy, [7]Cardiovascular Genetics Laboratory, Hatter Institute for Cardiovascular Research, Department of Medicine, University of Cape Town, South Africa,

[8]Department of Medicine, University of Stellenbosch, South Africa, [9]Chair of Sudden Death, Department of Family and Community Medicine, College of Medicine, King Saud University, Riyadh, Saudi Arabia, [10]Division of Cardiology, Samsung Medical Center, Sungkyunkwan University School of Medicine, Seoul, Korea, [11]Department of Cardiovascular Medicine, Okayama University Graduate School of Medicine, Dentistry and Pharmacuetical Sciences, Okayama, Japan, [12]Department of Cardiovascular Medicine, Medical Research Institute, Tokyo Medical and Dental University, Tokyo, Japan, [13]Division of Internal Medicine, Asao General Hospital, Kawasaki, Japan, [14]Department of Cardiology, Tokyo Metropolitan Hiroo Hospital, Tokyo, Japan, and [15]Department of Molecular Pathophysiology, Nagasaki University Graduate School of Biomedical Sciences, Nagasaki, Japan

[#]Corresponding Authors: Akinori Kimura, MD, PhD[1)] and Naomasa Makita, MD, PhD[2)]

1) Department of Molecular Pathogenesis, Medical Research Institute, Tokyo Medical and Dental University, 1-5-45 Yushima, Bunkyo-ku, Tokyo 113-8510, Japan. Phone: +81-3-5803-4905, FAX: +81-3-5803-4907, E-mail: akitis@tmd.ac.jp
2) Department of Molecular Pathophysiology, Nagasaki University Graduate School of Biomedical Sciences, 1-12-4 Sakamoto, Nagasaki 852-8523, Japan. Phone: +81-95-819-7031, FAX: +81-95-819-7911, E-mail: makitan@nagasaki-u.ac.jp

Expanded Methods

Supplemental Tables: 7 Tables

Supplemental Figures: 8 Figures

Expanded Methods

Subjects

Among the BrS patients analyzed in this study, 70 (13 Japanese and 57 Caucasian) patients developed a diagnostic BrS pattern only after the infusion of class Ic drugs such as flecainide, while the remaining 120 patients (72 Japanese, 3 Korean, and 45 Caucasian) had a spontaneous type I pattern in ECG. Family history of BrS and/or sudden cardiac death was observed in 60 (28 Japanese and 32 Caucasian) patients. Episodes of syncope, ventricular fibrillation, ventricular tachycardia, and/or implantation of implantable cardioverter defibrillator were recorded in 55 (41 Japanese, 3 Korean, and 11 Caucasian) patients. Because SLMAP mutations were found in Japanese, we analyzed 380 genetically unrelated Japanese healthy individuals selected at random.

Alignment of Amino Acid Sequences

Amino acid sequences of human SLMAP protein predicted from the nucleotide sequences (GenBank™ NM_007159) were aligned with those of chimp (NC_006490), macaque (NC_007859), mouse (NC_000080), rat (NC_005115), rabbit (NM_001082348), bovine (NC_007320), horse (NC_009159), dog (NC_006602), platypus (NC_001790902), chicken (NC_006099), xenopus (NM_001113814), and zebrafish (NM_200177).

Constructs for SLMAP, hNavβ1 and hNav1.5

We obtained cDNA fragments of human SLMAP3 by RT-PCR from human heart cDNA. Wild-type (WT) cDNA fragment of SLMAP3 with TM1 domain (from bp64 to 2490 of AF_100750, corresponding to aa1-808) and SLMAP3 with TM2 domain (from bp206 to 2641 of NM_007159, corresponding to aa1-aa811) were amplified, and equivalent cDNA fragments containing a G to A substitution in codon 269 (for Val269Ile mutation), a C to A substitution

in codon 288 (for His288Tyr variation) or an A to C substitution at codon 710 (for Glu710Ala mutation) were created by the primer-mediated mutagenesis method (Supplemental Table S3). The cDNA fragments of SLMAP were cloned into pEGFP-C1 for EGFP-SLMAP, pcDNA3.1 for pcDNA3.1-SLMAP, and pIRES-CD8 for pIRES-CD8-SLMAP. WT and mutant cDNA fragments of SLMAP1 with TM1 domain (from bp150 to 1229 of AF_304450, corresponding to aa1-359) and SLMAP1 with TM2 domain (from bp1556 to 2641 of NM_007159, corresponding to aa450-aa811) were obtained by PCR using the SLMAP3 constructs as templates. The cDNA fragments of SLMAP were inserted into the XhoI and EcoRI sites of pEGFP-C1 (for EGFP-SLMAP), into the BamHI and NotI sites of pcDNA3.1 (+) vector (for pcDNA3.1-SLMAP), and the XmaI and NotI sites of pIRES-CD8 (for pIRES-CD8-SLMAP). We also obtained cDNA fragments of hNavβ1 by RT-PCR from human adult heart cDNA, and the fragments were cloned into pcDNA3.1-myc, His-B to obtain myc, His-hNavβ1construct.

Expression of endogenous SLMAP

HEK293, tsA-201, and H9c2 cells were seeded onto poly-D-Lysine coated (for HEK293 and tsA-201) or collagen type I coated (for H9c2) 60mm dishes, respectively. 24 hr later, 0.8μg of EGFP-SLMAP3-TM1-WT were added into dishes with 1.6 μl of TransFectin lipid reagent (Bio-Rad). After 48 hr of the transfection, the cells were harvested. The aliquots of the cellular extracts were separated by 12% or 6% SDS-PAGE, transferred to a nitrocellulose membrane, preincubated with 5% skimmed milk in phosphate-buffered saline (PBS), and incubated with primary mouse anti-SLMAP monoclonal Ab (1:100; Santa Cruz Biotechnology, Inc.) followed by secondary rabbit anti-mouse (for monoclonal Ab) IgG HRP-conjugated Ab (1:1000; Dako A/S, Grostrup, Denmark).

Immunofluorescence Microscopy

HEK293 cells or H9c2 cells (4.0×10^5) were respectively seeded onto poly-D-Lysine 8-well

culture slides or collagen type I 8-well culture slides (BD Biosciences, CA, USA), and 24 hours later, the cells were transiently transfected with the combination of EGFP-SLMAP (0.075μg or 0.15μg) and L1-Flag-hNav1.5 (0.15μg) or the combination of EGFP-SLMAP (0.075μg), pcDNA3.1-SLMAP (0.075μg) and L1-Flag-hNav1.5 (0.15μg) with 0.6 μl of TransFectin lipid reagent (Bio-Rad, CA, USA). After 48 h of the transfection, the cells were washed with PBS, fixed in 4% paraformaldehyde for 15 min at room temperature (RT) and permeabilized by 0.15% Triton X-100 in PBS with 3% bovine serum for 20 min at RT. The cells were then incubated with the primary rabbit anti-Flag polyclonal Ab (1:250, Sigma, CA, USA) and secondary Alexa fluor 568 goat anti-rabbit IgG (1:500, Molecular Probes, OR, USA) in PBS with 3% bovine serum. All cells were mounted on a slide glass using Mowiol 4-88 Reagent (Calbiochem, Darmstadt, Germany) with 4-6-diamidino-2-phenylindole (DAPI, Sigma), and images were collected and analyzed with LSM510 laser-scanning microscope. To quantify membrane expression of Nav1.5, fluorescence intensity at the entire cell area and the plasma membrane region in the middle *xy* images of *z* series stack were measured, and the ratios of peripheral to total cell area fluorescence intensity were calculated. Analyses of labeled cells were performed using ImageJ software.

Silencing of Transfected SLMAP by Small Interfering RNA (siRNA)

Pre-designed siRNA for human SLMAP (siRNA ID: s15435) and non-silencing siRNA as a negative control were purchased from Ambion (TX, USA). HEK293 cells (4.0×10^5 or 4.0×10^4) were seeded onto poly-D-Lysine coated 60mm dishes or poly-D-Lysine 8-well culture slides, respectively (BD Biosciences). After 24 h, the cells were co-transfected with the combination of each 2 μg (for 60mm dishes) or 0.15μg (for 8-well slides) construct of each EGFP-SLMAP and L1-Flag-hNav1.5 and simultaneously transfected with the pre-designed siRNA or non-silencing siRNA at a final concentration of 30 nM using Lipofectamine 2000 (Invitrogen). After 48 h of the transfection, the cells were collected and subjected to brief

sonication in TNE buffer (1% Nonidet P-40, 1mM EDTA, 150mM NaCl, and 10mM Tris-HCl, pH7.8) containing a protease inhibitor cocktail (Sigma). After measuring total protein concentrations by BCA protein assay (Pierce, IL, USA), aliquots of the cell lysates were subjected to SDS-PAGE, transferred to a nitrocellulose membrane (Invitrogen), preincubated with 5% skim milk in PBS, and incubated with primary mouse anti-GFP monoclonal Ab (1:100; Santa Cruz, CA, USA), followed by secondary rabbit anti-mouse IgG HRP-conjugated Ab (1:1000; Dako A/S, Grostrup, Denmark). Signals were visualized by Immobilon Western Chemiluminescent HRP substrate (Millipore, MA, USA) and luminescent image analyzer LAS-3000mini (Fujifilm, Tokyo, Japan). The cells on 8-well slides were fixed and applied for immunofluorescence analysis as described above.

Electrophysiological Studies

The tsA-201 cells were transfected transiently with either WT or mutant EGFP-SLMAP plasmid or pIRES-CD8-SLMAP (1μg) in combination with pcDNA3.1-Nav1.5 plasmid (0.75μg) using Lipofectamine LTX and Plus Reagents (Invitrogen). The cells transfected with pIRES-CD8-SLMAP were briefly preincubated with Dynabeads M-450 CD8 (Dynal, Oslo, Norway) prior to the recordings. Sodium currents were recorded from the cells that were positive for EGFP or labeled with CD8-Dynabeads using the whole-cell patch clamp techniques. Currents and cell capacitances were recorded using Axopatch 200B amplifier (Axon Instruments, CA, USA) and series resistance errors were reduced by 60-70% using electronic compensation. Holding potentials were -120mV and pipette resistance was 1.0-1.5 MΩ. Bath solution contained 145mM NaCl, 4mM KCl, 1.8mM $CaCl_2$, 1mM $MgCl_2$, 10mM HEPES, and 10mM glucose, pH7.35, while pipette solution contained 10mM NaF, 110mM CsF, 20mM CsCl, 10mM EGTA, and 10mM HEPES, pH7.35. All signals were acquired at 20-50 kHz (Digidata 1332, Axon Instruments) with a personal computer running Clampex 8 software (Axon Instruments) and filtered at 5kHz with a 4-pole Bessel low pass

filter. Experiments were done at room temperature (22-24°C). Membrane currents were analyzed with Clampfit 8 software (Axon Instruments) and SigmaPlot (Systat Software Inc, CA, USA). The current-voltage relationships were fit to the Boltzmann equation, $I=(V-V_{rev})\times G_{max}\times[1+\exp(V-V_{1/2})/\kappa]^{-1}$, where I is the peak sodium current during the test pulse potential V. The parameters estimated by the fitting are V_{rev} (reversal potential), G_{max} (maximum conductance), and κ (slope factor). Steady-state availability was fit with the Boltzmann equation, $I/I_{max}=[1+\exp((V-V_{1/2})/\kappa)]^{-1}$, where I_{max} is the maximum peak sodium current, to determine the membrane potential for $V_{1/2}$ (half-maximal inactivation) and κ (slope factor). The time course of inactivation was fit with a two-exponential function: $I(t)/I_{max}=A0+A1\times\exp(-t/\tau_1)+A2\times\exp(-t/\tau_2)$, where A and τ are amplitudes and time constants, respectively. I and t refer to current and time, respectively.

Co-immunoprecipitation (co-IP) assay

HEK293 cells were transiently co-transfected with a combination of L1-Flag-hNav1.5 (2μg), EGFP-SLMAP3 (WT, -V269Y, -H288Y, or E710A) (2μg), and myc, His-hNavβ1 (2μg) to analyze their direct binding. Aliquots of the cellular extracts were collected for assessing the expression levels, and the remaining supernatants containing equal amount of proteins were used for the co-IP assay using the Catch and Release version 2.0 reversible immunoprecipitation system, according to the manufacturer's instructions (Millipore, Billerica, MA), with rabbit anti-flag polyclonal antibody (Ab) (Sigma). Eluted samples were separated by SDS-PAGE, transferred to a nitrocellulose membrane, preincubated with 5% skimmed milk in phosphate-buffered saline (PBS), and incubated with primary mouse anti-c-myc monoclonal Ab (1:100; Santa Cruz Biotechnology, Inc.) or mouse anti-GFP monoclonal Ab (1:100; Santa Cruz Biotechnology, Inc.) followed by secondary rabbit anti-mouse (for monoclonal Ab) IgG HRP-conjugated Ab (1:1000; Dako A/S, Grostrup, Denmark).

Legend to Supplemental Figures

Figure S1. Mutational analysis of *SLMAP* gene in BrS

A, Direct sequencing data for *SLMAP* exon 8, exon 9 and exon 21, in controls (upper panels) and patients (lower panels). **B**, Amino acid sequence alignments of SLMAP from various species around the Val269Ile (V269I), His288Tyr (H288Y), and Glu710Ala (E710A) variants.

Figure S2. Expression level of endogenous SLMAP in transfected cells with SLMAP3

EGFP-SLMAP3-TM1-WT was transfected to tsA-201, HEK293, and H9c2 cells, and 48hr later, the cells were harvested, and the lysates were subjected to WB analyses. Data from two independently transfected cells were shown for each cell line. Filters were prepared for 6% and 12% SDS-PAAGE to detect the expression of endogenous SLMAP3 and transfected EGFP-SLMAP3-TM1 (upper figure, 6% SDS-PAGE) and the expression of endogenous SLMAP1 and SLMAP2 (lower figure, 12% SDS-PAGE). Positions of SLMAPs and protein size markers are indicated on the left and right of figures, respectively.

Figure S3. Cell surface expression of hNav1.5 in H9c2 cells co-transfected with L1-Flag-hNav1.5 in the presence of SLMAP

H9c2 cells were transiently co-transfected with L1-Flag-hNav1.5 and EGFP-SLMAP3-TM1-WT (*a*, *b* and *c*), -SLMAP3-TM1-V269I (*d*, *e* and *f*), -SLMAP3-TM1-H288Y (*g*, *h* and *i*), -SLMAP3-TM1-E710A (*j*, *k* and *l*). The cells were permeabilized and stained with anti-Flag Ab (red; *b*, *c*, *e*, *f*, *h*, *i*, *k*, and *l*), and expression of EGFP-SLMAP is shown in *a*, *d*, *g*, and *j* (green). The images (*c*, *f*, *i*, and *l*) show enlarged images in the boxed region of *b*, *e*, *h*, and *k*. Scale bar, 5μm and 1.25μm, respectively.

Figure S4. Silencing of transiently expressed *SLMAP1* in HEK293 cells

A, HEK293 cells were co-transfected with L1-Flag-hNav1.5 and EGFP-SLMAP1-TM1-WT

(*a*, *b*, *e*, and *f*), -SLMAP1-TM1-E261A (*c*, *d*, *g*, and *h*), -SLMAP1-TM2-WT (*i*, *j*, *m*, and *n*), -SLMAP1-TM2-E261A (*k*, *l*, *o*, and *p*) in non-silencing (*a*-*d* and *i*-*l*) or pre-designed (*e*-*h* and *m*-*p*) siRNA, permeabilized by 0.15% Triton X-100, and stained with anti-Flag Ab (red, *a*, *c*, *e*, *g*, *i*, *k*, *m*, and *o*). Expression of EGFP-SLMAP1 was shown in *b*, *d*, *f*, *h*, *j*, *l*, *n* and *p* (green). Scale bar, 10μm. **B**, The PTAFI ratio of expressed L1-Flag-hNav1.5 in the transfected cells. Numbers of the analyzed cells are indicated at the bottom of each bar. The silenced expression of EGFP-SLMAP1 by pre-designed siRNA against human SLMAP (s15435) at a final concentration of 30nM was confirmed by the Western blot analysis as shown in the lowest panel. PTAFIs were compared between the cells transfected with non-silencing siRNA and with SLMAP-siRNA. **, $p<0.01$; ***, $p<0.05$.

Figure S5. Sodium currents recorded from tsA-201 cells co-transfected with Nav1.5 and SLMAP3-TM2 constructs

A, Representative sodium currents were recorded from transfected tsA-201 cells of pcDNA3.1-hNav1.5 with EGFP, EGFP-SLMAP3-WT, -SLMAP3-V269I, -SLMAP3-H288Y, or -SLMAP3-E710A, with TM2 domain. These traces were recorded with the whole-cell configuration as shown in the inset. **B**, Current-voltage relationship for peak I_{Na}. EGFP-SLMAP3-V269I and -E710A showed a significant decline of peak current densities by 51.9% and 40.7% (n=13 for WT, n=11 for V269I, n=13 for E710A) at -30mV, whereas EGFP-SLMAP3-H288Y (n=12) did not alter the peak current density. **C**, The voltage dependence of steady-state fast inactivation and activation recorded from the transfected cells of pcDNA3.1-hNav1.5 in combination with EGFP, -SLMAP3-V269I, -SLMAP3-H288Y or -SLMAP3-E710A with TM2 domain, were similar to that of the cells co-transfected with pcDNA3.1-hNav1.5 and EGFP-SLMAP3-WT, with TM2 domain. **D**, Recovery from inactivation assessed by the double-pulse protocol was nearly identical among WT, V269I, H288Y and E710A in SLMAP3. The-2 pulse protocol is shown in the inset.

Figure S6. Sodium currents recorded from tsA-201 cells co-transfected with Nav1.5 and SLMAP1 constructs

A, Representative sodium currents were recorded from transfected tsA-201 cells of pcDNA3.1-hNav1.5 in combination with EGFP-SLMAP1-WT or -SLMAP1-E261A, with TM1 or TM2 domain. These traces were recorded with the whole-cell configuration as shown in the inset. **B**, Current-voltage relationships for peak I_{Na}. EGFP-SLMAP1-E261A showed the significant decline of peak current densities due to EGFP-SLMAP1-E261A by 38.7% (n=8 for WT, n=14 for E261A in TM1 isoform) and 39.9% (n=11 for WT, n=13 for E261A in TM2 isoform) at -30mV. **C**, The voltage dependence of steady-state fast inactivation and activation of the cells co-transfected with pcDNA3.1-hNav1.5 and EGFP-SLMAP1-E261A, with TM1 or TM2 domain, were similar to that of the cells co-transfected with pcDNA3.1-hNav1.5 and EGFP-SLMAP1-WT, with TM1 or TM2 domain. **D**, Recovery from inactivation assessed by the double-pulse protocol was nearly identical between WT and E261A in SLMAP1. The-2 pulse protocol is shown in the inset.

Figure S7. Sodium currents recorded from tsA-201 cells co-transfected with hNav1.5 and SLMAP1 constructs

A, Representative sodium currents were recorded from transfected tsA-201 cells of pcDNA3.1-hNav1.5 with pIRES-CD8, pIRES-CD8-SLMAP3-WT, -SLMAP3-V269I, -SLMAP3-H288Y, or -SLMAP3-E710A, with TM1 domain. These traces were recorded with the whole-cell configuration as shown in the inset. **B**, Current-voltage relationship for peak *I*Na. pIRES-CD8-SLMAP3-V269I and -E710A showed a significant decline of peak current densities by 47.7% and 52.7% (n=13 for WT, n=9 for V269I, n=11 for E710A) at -30mV, whereas pIRES-CD8-SLMAP3-H288Y (n=11) did not alter the peak current density. **C**, The voltage dependence of steady-state fast inactivation and activation recorded from the

transfected cells of pcDNA3.1-hNav1.5 in combination with pIRES-CD8, -SLMAP3-V269I, SLMAP3-H288Y or -SLMAP3-E710A with TM1 domain, were similar to that from the cells co-transfected with pcDNA3.1-hNav1.5 and pIRES-CD8-SLMAP3-WT, with TM1 domain. **D**, Recovery from inactivation assessed by the double-pulse protocol was nearly identical among WT, V269I, H288Y and E710A in SLMAP3. The 2 pulse protocol is shown in the inset.

Figure S8. Binding assay between SLMAP3 and hNav1.5

HEK293 cells were co-transfected with flag-tagged hNav1.5 (L1-Flag-hNav1.5), myc-tagged hNavβ1 (myc, His-hNavβ1), and WT or mutant/variant (V269I, H288Y, or E710A) EGFP-tagged SLMAP3-TM1 (EGFP-SLMAP3). Cell lysates were prepared and subjected to WB analyses after immunoprecipitation. Upper lanes; amounts of input proteins, flag-tagged hNav1.5, myc-tagged hNavβ1, and EGFP-tagged SLMAP3, in the co-IP assay, detected by anti-flag, anti-myc, and anti-GFP antibody, respectively. Lower lanes; amounts of myc-tagged hNavβ1 and EGFP-tagged SLMAP3 after the immunoprecipitation with anti-flag polyclonal immunoglobulin (Flag-poly) or control rabbit immunoglobulin (rabbit IgG), detected by anti-myc and anti-GFP antibody, respectively.

Table S1. Nucleotide sequences of the primers used for the mutational analysis of *SLMAP*

Analyzed Region	Forward primer (5' to 3')	Reverse primer (5' to 3')
Ex1	TCCGGATCCGGAGGAACTC	CCTGCATACATTAGTCCTCTC
Ex 1*	TTAAAATTTTGGGTGGGAT	GCATACATTAGTCCTCTCAG
Ex2	GCAATAGTTGGCAAAGCTGG	CGCTTTCACAAGCATGTAATG
Ex3	ACAAGATGAGTTTCTCCAGGG	AGCAGTACACCATCACCTAG
Ex 3*	TATGAGAGGTGTGAAGTTT	GAAGCAGGTATTAGCAGTA
Ex4	GTGTAAGATATTCTGGTGCTC	CAAAGCAACATAGCTGAGTCAG
Ex5	AAGGCTATATTGCCTTTGTGC	CATGCCTGGCCCTAATTCTGC
Ex6-7	GCTGAAAATTGATCACTCCTC	AATGATAGTCAAAGAAATGATGTTAC
Ex 6*	TCAAGTGGGATGTAATATG	ACTTTGTCTTTGTTTGCTA
Ex 7*	TATCTTTTGTTGTCAGTAG	AATGTATGAAGTTTTTAGC
Ex8	CTTTAGTTAATACAGGGCCAG	AAGTATCCTGGAATGCTTGAG
Ex9	CCAGGGCAGATGTTGATTTAG	AAGCTATCTAGTGTGTTAGGG
Ex 9*	GTTGATTTAGAATAGTCCATAG	AGGGATTATTAGCTTAACATACT
Ex10	TAAGTGAATAAAGGCATTCCTGG	CTCCTGAAGATGTTCTAACCG
Ex11-12	CAAGGTAAGTAGCTAATCCAG	ACCCTGAACTCCTTATCCTG
Ex 11*	CACCAATGAAAGGCTAACAG	AAAATGCAGTGTGAGACAGT
Ex 12*	TACACTTGAGACCACATTTA	CCAAACACTTAAAACCCTGA
Ex13	GCTGTTGGTTTTCAAAGACAGC	AGATCCTCATTTTACCTCTCAC
Ex14	GAATGTGTTACACTGCCCAG	CTGGCTTGCTATTTTGTGAGC
Ex 14*	TCCCCTTCCAGATTCAAGT	CCAAAAGAACTGTCAAAAAA
Ex15-16	GCATTCATAGCCTGAAGCAG	GCAAAGGGTGATTTGATACCC
Ex 15*	CCTGTAGATTTTGAGCATTC	TCCACTCACATTGACCTAT
Ex 16*	ACTACTTTCAACTACCCGA	GCTACTTTACAGAACCTATC
Ex17	TGCAAACATGAGAGAGATTACC	CCACACATCCCTAAAGAACC
Ex18	AGCTGCTCAACTCTGAGTAC	CCTCCATTCCTTTTGAATCAC
Ex19	TCTGACAACCCAGGTTATGC	AGTTAAGAAGTTATCATTGTCAAAAG
Ex 19A*	TCTGACAACCCAGGTTATGC	CCTTTGCTGCTGCTTGATG
Ex 19B*	GCTTAGTGCCCGAGATGAA	AGTTAAGAAGTTATCATTGTCAAAAG
Ex20	GGCAAAAAGTATGTTCTCCTC	GGGCTGAACATTTGCTCCTG
Ex21	GAAACTGGACTTCCTTCTGTG	GTCCAACCATAATTGGGCTC
Ex22	GGATCTGGCGTATAAACCTG	CAATCTCTCATGTGCCTCTC
Ex23	GGGGTCTGAATCCTCTTATC	TGTGTGTTCTTGCCATGCAC
Ex24	TATTCAGGACTCTCTGGAACC	ATGAGTGTGATGCCAGCTTC
Ex 24*	AGGACTCTCTGGAACCAAGGG	TATTCTTGTACTTCTGCTGT

* Alternate exon primers designed to make all exons compatible with DHPLC mutational analysis.

Table S2. Nucleotide sequences of the primers used for the mutational analysis of known BrS genes

Gene and region	Forward primer (5' to 3')	Reverse primer (5' to 3')
SCN5A		
Ex1	GAGCACCACGTGCGGAGCCCTG	GCTCTCTGGGGCACTGATC
Ex2	CAGCACAGCCACCCCCAGGA	CCCCATATGGAGGCCAGGC
Ex3	CAAGGGCTCTGAGCCAAAAG	CGCTACTCTCACTCCTAAAC
Ex4	GTTTATTGTCTGGTAGCACTG	ACCGCCATGGGTAAGTTCCTG
Ex5	CTCAGGCCTCCCTAAGAAAC	TGTGGACTGCAGGGAGGAAG
Ex6	CAGATCTCAGCTACAAGTGAC	TCTGGTTGACAGGCACATTCG
Ex7	TTATTCTGTCCCCACCTCTG	GCTGCAGAGCAAGTTCGCAC
Ex8	GAAGGAAGACCGCTAGTGAG	CAAAAGAAGGCCTCGCTGTC
Ex9	GTGGGGCATAAACTGGGTTG	CTCAGAAGCAAGGGTCCTTG
Ex10	CTAGGTGACTTGGAAATGCC	GGCATATACCCCACCTATAG
Ex11	GCAAGTCCACTTACTGATAGG	ACCCACCCTGGAAAAGCTAG
Ex12	CTAACCCCACATCCCCTCTT	TATTTTTGGACTTGGCAC
Ex13	TCATCCTATCCCTGTGGCATC	GTCAGGCTGGGATAAAGATG
Ex14	GTCATCTCCCAGAGCAAGTC	CCAGGATGCCCATTTGAGAG
Ex15	CAGGCTGGAGAAGAGAGCTG	GTGCCGAGCCTTCCACACCC
Ex16	CAGGAGCTAGAGAGAGTGAG	GCTGGGTAGATGAGTGGATG
Ex17	CCTCAGTTTCCCCATCATAG	AGCTGCTTTGAGAGAGGCTG
Ex18	GGCAATGCCCCAGATGCATG	CAAATGCAGGCATGCACCTC
Ex19	TCGAGGCCAAAGGCTGCTAC	GAGGTGGGCAGATATCTAAG
Ex20	CAACCTTCTGCCATTAGATG	CAGTTTCTGACCTGACTTTC
Ex21	CAACAGAGCAAGACTGTCTC	CCTCTCTGCCTGCCCCACAG
Ex22	ACCAGAAGGCCTACTGTCTG	CCATAGGACATCAGAAGCAC
Ex23	ATTCTTTCTTGGGGTGGCAG	CATGGGTGATGGCCATGCTG
Ex24	TTCATCTGTCCAGACCAGAG	CAGATGCAGACACTGATTCC
Ex25	TAGACAGCCCTCTGCCTCTG	CTCTAACCAGCAGGAGCAAG
Ex26	CTGGCATCCTCATCAAGAAG	CCATGTGGCACGAAAGCTTC
Ex27	GAGGCAGCAACAGGCATTTG	GTACATGGCATTCAGCAGAG
Ex28-A	GCTCCTTGCCATATAGAGAC	AGTCAGACAGGACCGAATAC
Ex28-P	GTGAGGACGACTTCGATATG	AGGCTGCTTTTCAGTGTGTC
CACNA1C		
Ex1	CTGACTTCTTTCTCTGCCCAC	AAAGGGAGGTGTCAGGGAAGG
Ex2	GCCTCTGATTTGCACCTAGAG	ATCCACTTCAAGGCTCCTGTG
Ex3	GAGCTGTCTGTGGAAAGTAGG	CGGTCAAAGTTCTGTGCTGAC
Ex4	GCGTGTTGCAAACTACTGCTC	CCCACTGTGATTTCCAGATGC
Ex5	TCTAGTTCACACCATGCCTCC	AGGTATTACCTTGGGCCACCC

Ex6	ATGGTGCTGCATCTTGGGTTG	CACCTTCTGCCTGTGGTTATG
Ex7	ACTGTATTTCCTTTCCCTGCC	GCATGTGAACTTCAGAGACAC
Ex8	TGTGAGAATGAGGCACGATGG	TAAAAGGGTGCAGCTTCCCAC
Ex9	CCAGGCATTTTGTCTAAGGAC	TCACCCATGCCAAAGCTGCAG
Ex10	CAAGCTCTCTCTGCTGAGGAG	AGGCTAGCAGTCAAGCCTCTC
Ex11-12	TGGAGAAAGGAAGATGGACTC	GTGGAAGGTACTTACAGAGGG
Ex13	TAGGAAGGTCTCTGAAAGTGG	AGTCTCCATCCAGAGGTTCAG
Ex14	CAAGCAGCAGTAAGACTTCAG	TGATGTCAGCAACAGAAGCTG
Ex15-16	AACATCCACTGACCTCTCTTC	TTCCAATTTCAGGCTTGGGAG
Ex17	AACTCTTTTCTTGGCACCATAG	TGAGGACACAGAACCAAGAAC
Ex18-19	TTCACCTGTCAGGACATTCCC	TCGTTTGTACTATATCTGCCAG
Ex20-21	CTGGGCTATGGAGATGCTCAC	AATATGACCTCCAGAGGGAGTG
Ex22	AGGTCACACAGCCAGTAAGAG	GCACAGGTCCCTCAAAAAGAC
Ex23	CACAGTGTGTGGTCTCATCAC	TTGGTGACCAGGAAAGCGATG
Ex24	TCAAGGAAGGTCTTGCTGAGG	TCTGCCTTCAATACCTGCACC
Ex25-26	CCTGGACGATGATTCTGATGG	ATGAGTGTTAGAGCAGGCACG
Ex27	CAGCCAAGACCTAGAATACCG	AATTACCACCCCAAGGAAAGC
Ex28	TGAGGTCTGTATTTCTCGGAG	CCTTGTGTCAGCTGTGTTCTG
Ex29	ATAGCTGATGGCTGCAGAGAC	GGAATGTGGTGCTGGGAACTG
Ex30	AGACCCCTGAAGAGACCATTG	CCATGCAGGTGTGTGTGTATC
Ex31	CAGAGCATTCAGGGAATGATG	TGACCATGAGCTGCAGAGATG
Ex32	GTTGGCTTCTGCCATCAGTAG	ATTGATCCACCCAGTGTTGGC
Ex33	GCAGTGTTGCCCATATGAGTG	AATTTAGAGCTGGAAGGACCC
Ex34	AACCATATCACTCTGCCACGG	GTTCCCTTGAGCACTTTGCAG
Ex35	ATCTGTGGCTTCCTACCTTAC	GATGCTTCCGCATTCTAAGGG
Ex36-37	AGTTCAACTGAATTCCCCTGC	AAGTAGCCCTTTCCTCTGGTG
Ex38	CCAGGCATGAAGAAGGTCCTC	TCTGATCAAGGGCAGGACTTG
Ex39	CGTGTGTGATGCTTTACTTGC	GAGATGAAAGAGGCGGTGCAG
Ex40-41	GGATCAGAGCAAAGTGCTTTC	CTTCAGGATTTGTCCGTCACC
Ex42	AAGCAGTGCTTGCTCAGAAGC	AATTTGGCAAGAGCCAGGTGC
Ex43	CCCAAGTGACCTACCAGATAC	GAGAACAGTGAGGCACTTCTG
CACNB2		
Ex1	TCTGCTTCCGAAAAGCCAGTG	ACAGGCAAACCTTGGCAAGTG
Ex2	GCCTACATTCCTGTTAAAGGG	AAACAGCACCGTCTTCACTTC
Ex3	CTAACTGCTGTGTCGATGAG	TCCCACAGGTGGTCTATCAG
Ex4	GCAGAGGGGAAACCAACAATG	TATACAACTGCAGCGATGTGC
Ex5	CTCTCGACTGAAAATAGTGTG	ACCATATTACCAGCCTCCTTG
Ex6	AATCAGAGACCATCATGTGGC	CCAAAAGGGCATGCTCACTTC
Ex7	TGTGTTGAGCACTCATGATAG	GCAGACAGTCAACAGGACTAG

Ex8	CCAGTGCCTCATATTATGGAG	TAGGAGGCAGCATCACAAAG
Ex9	TATTGCCACTCTTTCCAGATG	TCTCTTGGAATCACACGCATG
Ex10	TTGGGGCATACACTTCTATCC	GTCTTCTCATCATCAACATCG
Ex11	GACCTACTCACCTTTCTGTTG	TCTTGACTATCATGTCTCCTC
Ex12	CCATCTATTATAAGCCCCTTG	GAGCTAAGACCATACCACTG
Ex13	AAAGGGGTGCAGCTCATGAG	TTGGATCCTAGAGGTGTCAC
Ex14	AGGACTCTGCTTGAATGCAC	ATACTCTATCCATGCTATTGC
GPD1-L		
Ex1	AAGGCTGAACAGGCGGAGGTG	TGCCCAGCCCAGCAACGAGGTC
Ex2	AGGCTCAGTGTTTGAATCAG	GTTCCAAAACCCAAGTGCTG
Ex3	GGTCAGTGAGTGAAACCTTG	TCACTGCTGCTGCTAGTCTG
Ex4	AGCTGTACATAGGCAGTATAG	GCCCAACTAAGGAATGTTAAG
Ex5	ATGATCACCTCGATTGGAAAC	TCACTATTCTTCGCTGATGTG
Ex6	AAGATGGAGCCAATGTCCCTG	GCTGGCATGAAATCTCCACTG
Ex7	CCTGTAATCCCACCACTTTGG	TAGTCTAGCTCATCTCCGTGG
Ex8	CTGAGGTAAATCCAGTGGCC	CAAGTCCTGGTTTCCACGTG
KCNJ8		
Ex1	GTTTCCCTCGTGCAGGAGGAC	ACCCCTGCCTCATCCCACTAC
Ex2	GAAAATGAAAAGCTCAGCTTG	AAGGACACATTATTGTGTTCC
SCN1B		
Ex1	TCTCGCCCCGCTATTAATAC	GCACAACTTCTGAAGCTGAC
Ex2	CTAGCATCCAGTCCTGTCTG	ATCCAGGTCAGCAATCACAG
Ex3	CTGTGTGCCATCTGTGTTTG	TGTCCACTGCCTGCCATCTG
Ex4	CTCACACAGCAAGCTCACAG	CTGGGTAGTACTGAGAGATG
Ex5	AGACTCCTTCTCTCTCTAAC	ATTACGGCTGGCTCTTCCTTG
SCN3B		
Ex1	AGTTCGTCCCAAAGGGTTTC	TCTTTTCTGTCACCAACGAC
Ex2	GGTTGGCCTCATGACTCTTC	AGCCAGTGTTTGCTAGCTTG
Ex3	TTCTCTGCCCTGTCCCTAAC	GTGGAAAACTGCTGTCCTAC
Ex4	GAGTCAGGATTTGGAATACC	TGCTTAGCACCTCACCTGTG
Ex5	TGTAGATCCTTGCTCCTGTG	TTGTACAACCTGCCATCCAC
KCNE3		
Ex1	TTTGAGCTGCAGGTGACAGAG	GCAGTCCACAGCAGAGTTCTG
MOG1		
Ex1-3	GCGGAGCCAAATCTTAAAGG	GCCCTTCCAGGACATTACAC

Ex4-5	GTGTAATGTCCTGGAAGGGC	AGTCCCCAAGTTCTCAGCAAC
HCN4		
Ex1-A	ACTCGGAGCGGGACTAGGATCCTC	GAGTCATGCAGGTGTCCGTGA
Ex1-P	TCACGGACACCTGCATGACTC	CAAGGCAGGAAAGTTAACTC
Ex2	TTCTCTGTCCCAGATGCTGTC	GCCACAATCTGACAGCCTATG
Ex3	AAGACCTAGACTGACGCCTTC	ATGCTGGAACTCAGAAGTTCC
Ex4	AGTTAGGTTGAGGTGAGGAG	TCACACTGGGAGTTCCGATC
Ex5-6	AAGGAACCAAGTTTAGCCAG	CTCTGTCCCCTCGGTATCTC
Ex7	AAGAGGCATCCAGTGTGGCC	CTGGCTTAGGCATAAAGGAGC
Ex8A	GTCTGCACCTGATCTCCTTC	CTACGCCAGCTGATGGTGTG
Ex8P	CACTCCTGCCCTCATCCAGCTCC	TCACATTAAACCTGAAGGAAG
KCND3		
Ex1-A	CCCAGGGTTTGCTGAACTAAC	CTCCACCACGTTGGTGATGAC
Ex1-P	CCTGGTCTTCTACTACGTGAC	GTTTCAGAGGTCATCCAGCTG
Ex2	GTGAATGATTGGCAGGGAAG	TGTGAGGAGCTCTAGTCCTG
Ex3	ATCAGGTGTCACCTGGGAAG	GTCCTCCTTGGGGTTCATAC
Ex4	TGCCCTTTGACCTTTAGTGG	GACAGACTTTGACTTCTGGC
Ex5	GCTGGAATGTACAATCAATGG	AGAAGAATCAGCAGCACATGC
Ex6	CTTCAAGGTCCAGAACAGAG	CTAGAGGATCCTCAAGGTTC
Ex7	ATCCTCCTAGTTACCACGAG	AGTGACCACCCACCAACATG
KCNE5		
Ex1	AGCTGGGTGCTACCGCTGTTTC	CAGGGATGAGCGAGATGAGGAG

Table S3. Nucleotide sequences of primers used in the construction of SLMAP plasmids

Name	Sequence (5' to 3')
SLMAP1-XhoF	AGCTCGAGAAATGGATGAGCAAGACCTAAATGAG
SLMAP3-XhoF	GTCCTCGAGCGATGCCGTCAGCCTTGGCCATCTTC
SLMAP3-EcoR	GGAGAATTCTCATGGAGAAGCTCTGGCCAGACC
SLMAP3-805MF	GAAAATTGAAGTGATTAG
SLMAP3-805MR	AAGTTTTCTAATCACTTC
SLMAP3-862MF	AGATGAATGTACCTATCTG
SLMAP3-862MR	TTCTTTCAGATAGGTAC
SLMAP3-2129MF	GATCCTTGAAAGCACAGC
SLMAP3-2129MR	AGATGCTGTGCTTTCAAGG

The GFP-tagged SLMAP constructs were obtained as follows. First, PCR amplification with a primer pair, SLMAP3-XhoF (sense) and SLMAP3-EcoR (antisense), was performed using genomic DNA as templates. The PCR product was then excised by digestion with XhoI and EcoRI and cloned back into the Xho1-EcoRI-cleaved pEGFP-C1 to obtain GFP-tagged SLMAP3-WT constructs. Second, for the construction of mutants by primer-mediated mutagenesis, we used GFP-tagged SLMAP3-WT constructs as templates and three sets of primer-pairs, for Val269Ile; SLMAP3-805MF and SLMAP3-805MR, for His288Tyr; SLMAP3-862MF and SLMAP3-862MR, and for Glu710Ala; SLMAP3-2129MF and SLMAP3-2129MR. The introduction of mutations was confirmed by sequencing. As for the SLMAP1 constructs, PCR amplification with a primer pair, SLMAP1-XhoF and SLMAP3-EcoR, was performed using GFP-tagged SLMAP3-WT or -E710A as templates. The PCR products were excised by digestion with XhoI and EcoRI and cloned back into pEGFP-C1 to obtain GFP-tagged SLMAP1 constructs.

Table S4. ECG findings in the proband patients with V269I and E710A.

Sex	Age (y.o.)	Mutation	ST elevation	PR duration (msec)	QRS duration (msec)	QT (msec)	QTc* (msec)
Male	46	Val269Ile	Saddle-back	160	100	400	421
Male	57	Glu710Ala	Coved	150	110	390	407

*: QTc were calculated by Bazett's formula.

Table S5. Relative cell surface expression of hNav1.5 in HEK293 cells expressing L1-Flag-hNav1.5 and SLMAP constructs

A) with SLMAP3 constructs

	PTAFI ratio	n
WT-TM1	0.564±0.022	12
V269I-TM1	0.367±0.029*,†	10
H288Y-TM1	0.585±0.030	10
E710A-TM1	0.372±0.017*,†	8
WT-TM2	0.538±0.020	12
V269I-TM2	0.398±0.018*,†	10
H288Y-TM2	0.557±0.029	10
E710A-TM2	0.411±0.019**,†	12

*: $p<0.001$; **: $p<0.01$ *versus* WT

†: $p<0.001$ *versus* H288Y

B) with SLMAP1 constructs

	PTAFI ratio	n
WT-TM1	0.533±0.028	10
E261A-TM1	0.401±0.017*	13
WT-TM2	0.591±0.039	10
E261A-TM2	0.413±0.019**	7

*: $p<0.001$; **: $p<0.01$ *versus* WT

C) with SLMAP3-TM1 constructs

EGFP-SLMAP	(μg)	pcDNA3.1-SLMAP	(μg)	PTAFI ratio	n
WT	0.075			0.549 ± 0.039	10
V269I	0.075			0.332 ± 0.040*	10
H288Y	0.075			0.532 ± 0.018	10
E710A	0.075			0.361 ± 0.035*	10
WT	0.075	V269I	0.075	0.311 ± 0.028*	10
V269I	0.075	WT	0.075	0.324 ± 0.034*	10
WT	0.075	E710A	0.075	0.323 ± 0.023*	10
E710A	0.075	WT	0.075	0.343 ± 0.029*	10

*: p<0.001 versus the cells transfected with 0.075μg of EGFP-SLMAP-WT

Table S6. Relative cell surface expression (PTAFI) of hNav1.5 in HEK293 cells expressing L1-Flag-hNav1.5 and SLMAP constructs in the presence of siRNA

A) with SLMAP3 constructs

SLMAP3 constructs	with non-silencing siRNA		with SLMAP-specific siRNA	
	PTAFI ratio	n	PTAFI ratio	n
WT-TM1	0.537 ± 0.021	12	0.550 ± 0.027	10
V269I-TM1	0.396 ± 0.016	10	0.553 ± 0.022**	10
H288Y-TM1	0.513 ± 0.006	10	0.542 ± 0.023	11
E710A-TM1	0.416 ± 0.026	12	0.538 ± 0.020***	10
WT-TM2	0.574 ± 0.026	12	0.528 ± 0.020	11
V269I-TM2	0.385 ± 0.016	10	0.574 ± 0.021*	10
H288Y-TM2	0.544 ± 0.041	10	0.569 ± 0.026	11
E710A-TM2	0.376 ± 0.021	8	0.527 ± 0.019***	10

*; $p<0.001$, **; $p<0.01$, ***; $p<0.05$ versus non-silencing siRNA

B) with SLMAP1 constructs

SLMAP1 constructs	with non-silencing siRNA		with SLMAP-specific siRNA	
	PTAFI ratio	n	PTAFI ratio	n
WT-TM1	0.553 ± 0.032	10	0.520 ± 0.030	10
E261A-TM1	0.411 ± 0.018	13	0.516 ± 0.030***	10
WT-TM2	0.542 ± 0.024	10	0.569 ± 0.030	10
E261A-TM2	0.432 ± 0.023	7	0.547 ± 0.037***	10

***; $p<0.05$ *versus* non-silencing siRNA

Table S7. Electrophysiological properties of transfected tsA-201 cells of pcDNA3.1-hNav1.5 and pIRES-CD8-SLMAP3-TM constructs

	WT	n	V269I	n	H288Y	n	E710A	n	WT+V269I	n	WT+E710A	n	pIRES-CD8	n
Current density at -30mV (pA/pF)	-284.5 ± 39.7	13	-148.8 ±24.1†	9	-248.0 ± 27.7	11	-134.7 ± 20.6†	11	-161.1 ± 22.9†	13	-165.4 ± 30.3†	9	-305.1 ± 31.9	13
Voltage dependence of inactivation ($V_{1/2}$, mV)	-81.56 ± 1.36	13	-81.35 ± 1.17	9	-83.43± 1.37	11	-82.75 ± 2.23	11	-81.38 ± 0.97	13	-82.66 ± 1.58	9	-81.60± 1.53	13
Voltage dependence of activation ($V_{1/2}$, mV)	-44.69 ± 1.29	13	-44.88 ± 1.77	9	-45.83 ± 1.18	11	-47.0 ± 1.87	11	-43.49 ± 1.59	13	-47.1 ± 1.82	9	-45.7 ± 1.79	13
Time required for e^{-1} fraction recovery (msec)	5.43 ± 1.44	13	6.55 ± 1.21	8	5.71 ± 0.78	11	6.12 ± 0.92	10	5.94 ± 0.82	12	6.99 ± 1.51	9	5.79 ± 1.22	13

† : $p<0.05$ versus WT

Supplemental Figure S1

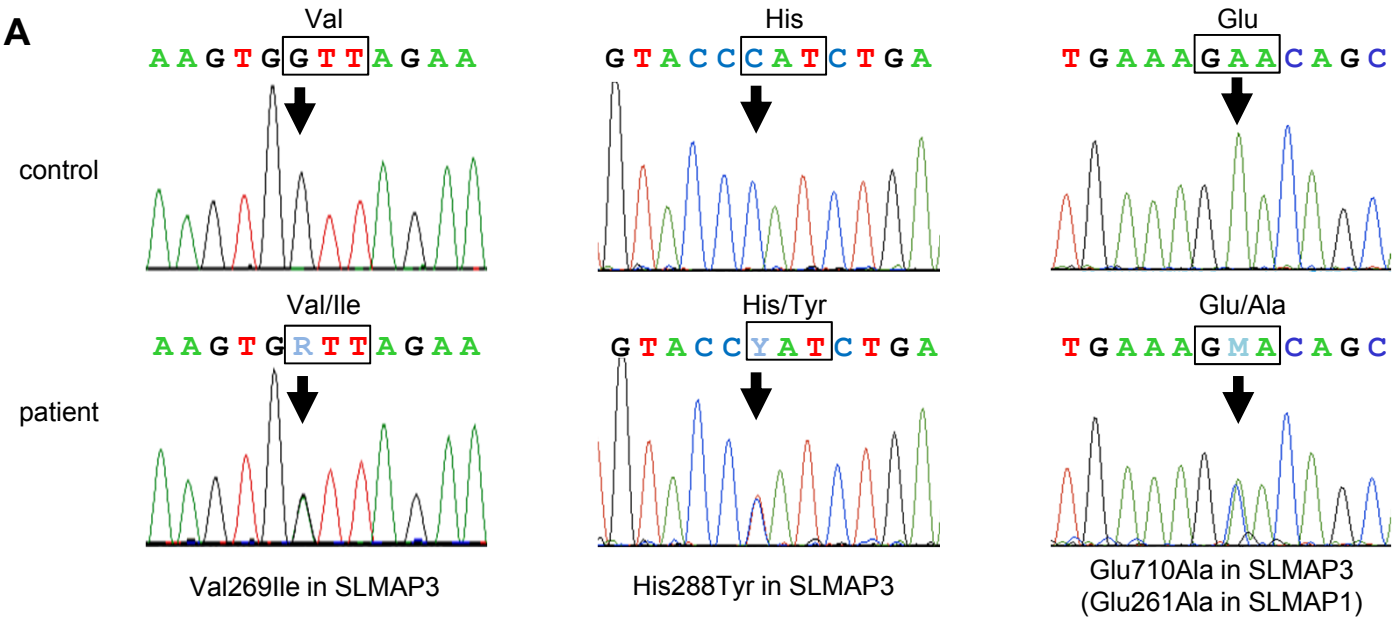

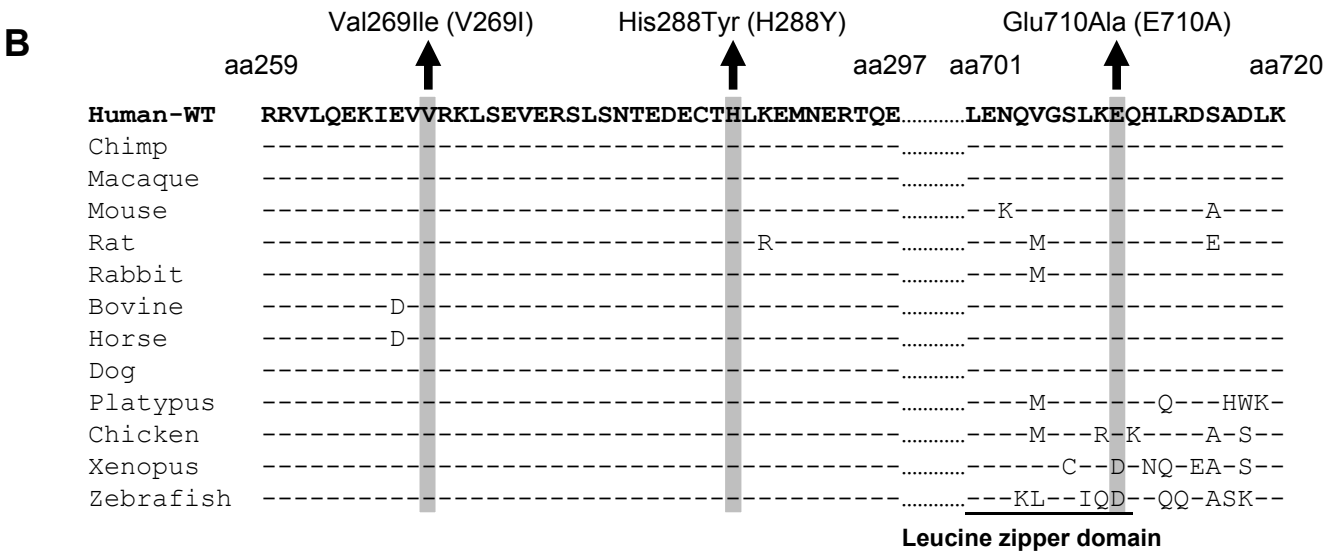

Supplemental Figure S2

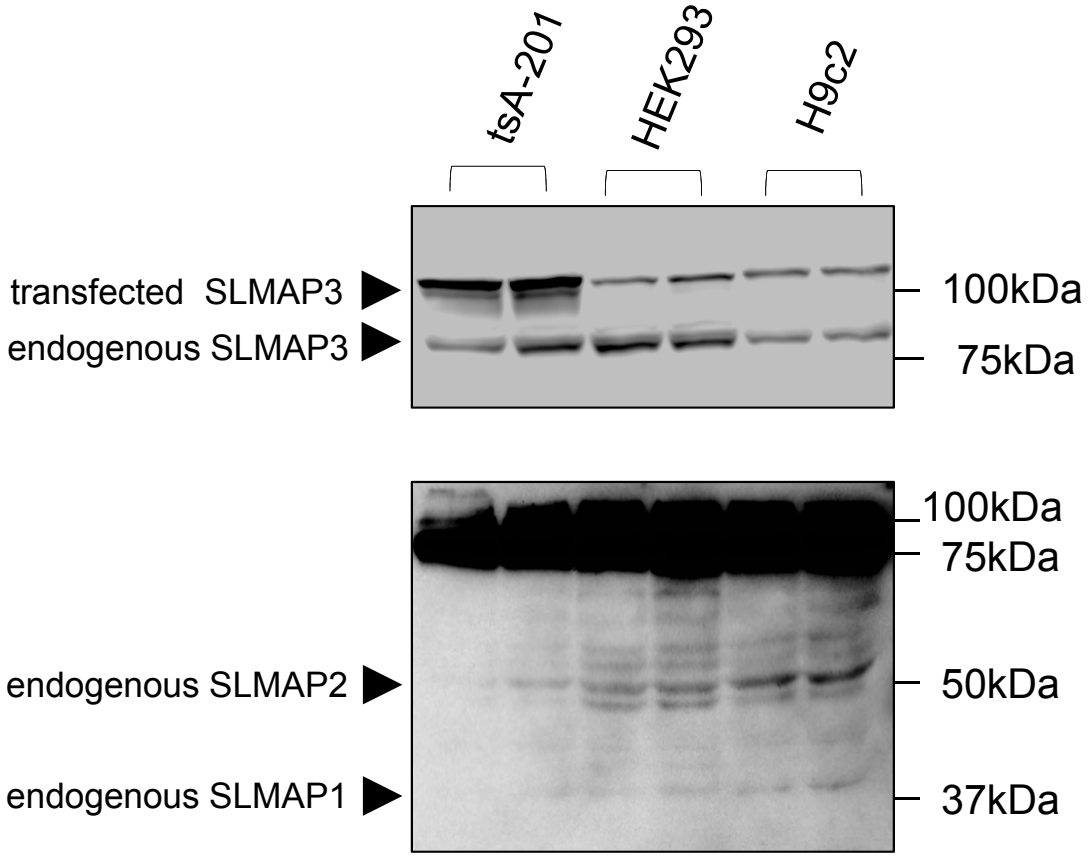

Supplemental Figure S3

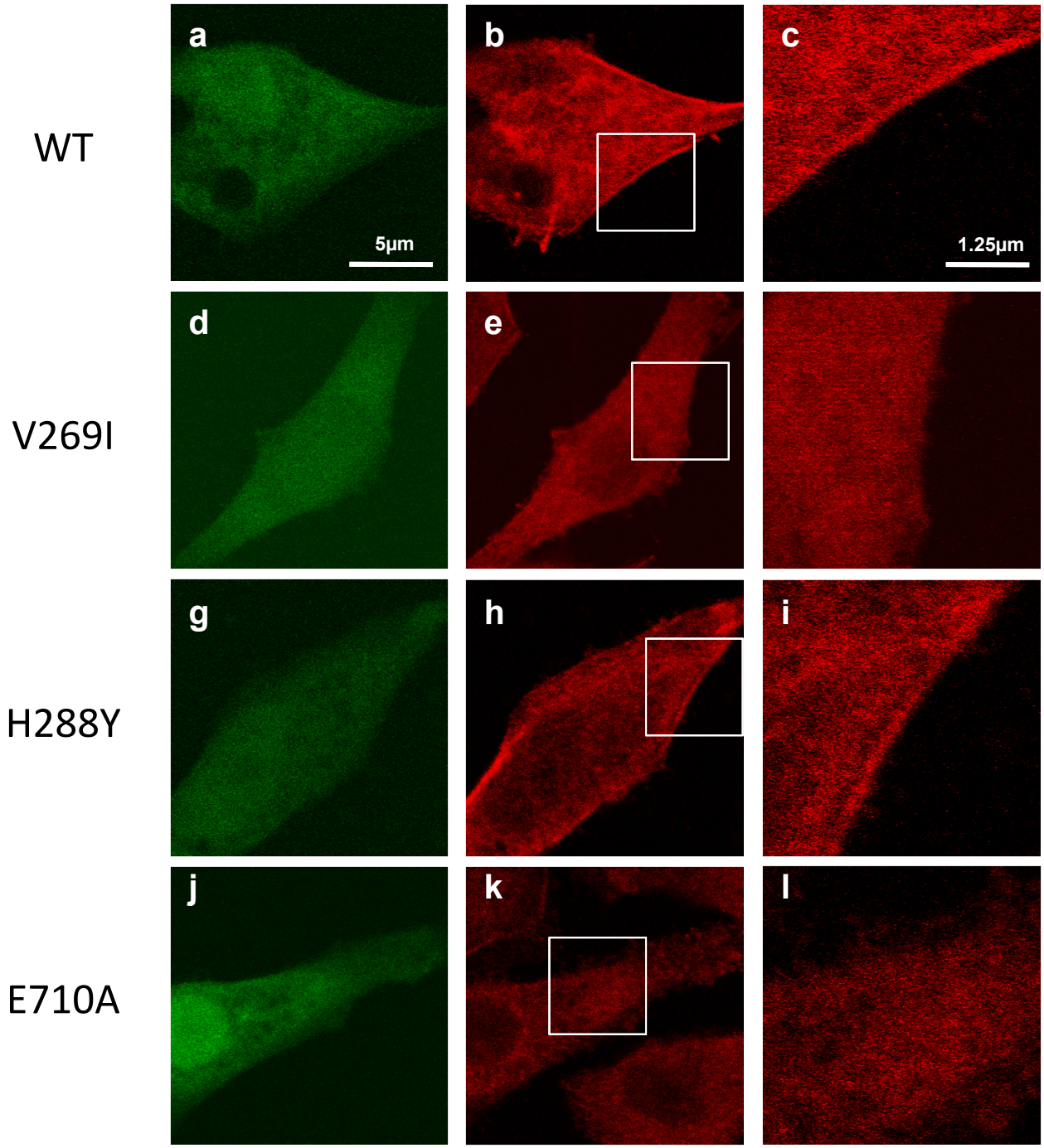

Supplemental Figure S4

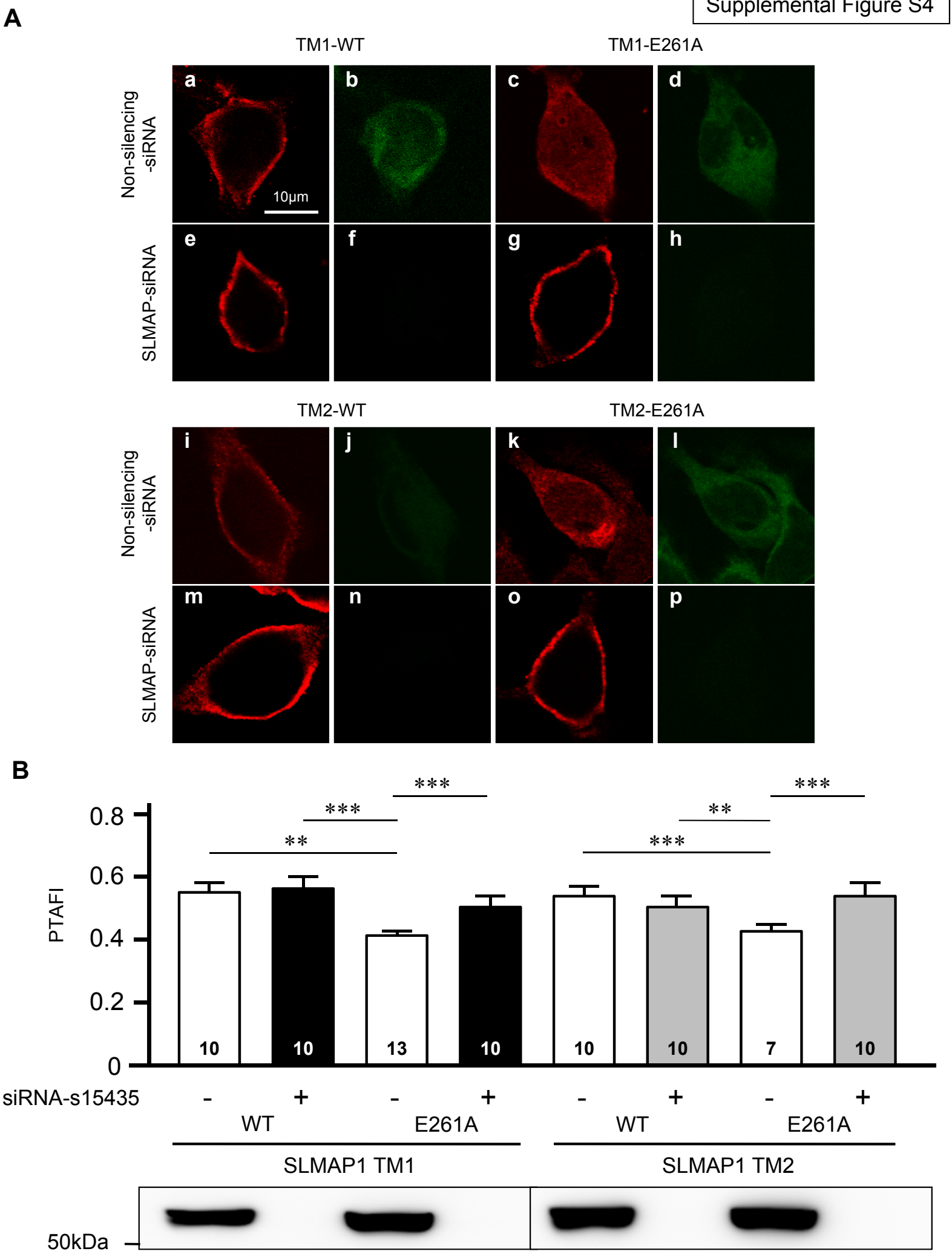

Supplemental Figure S5

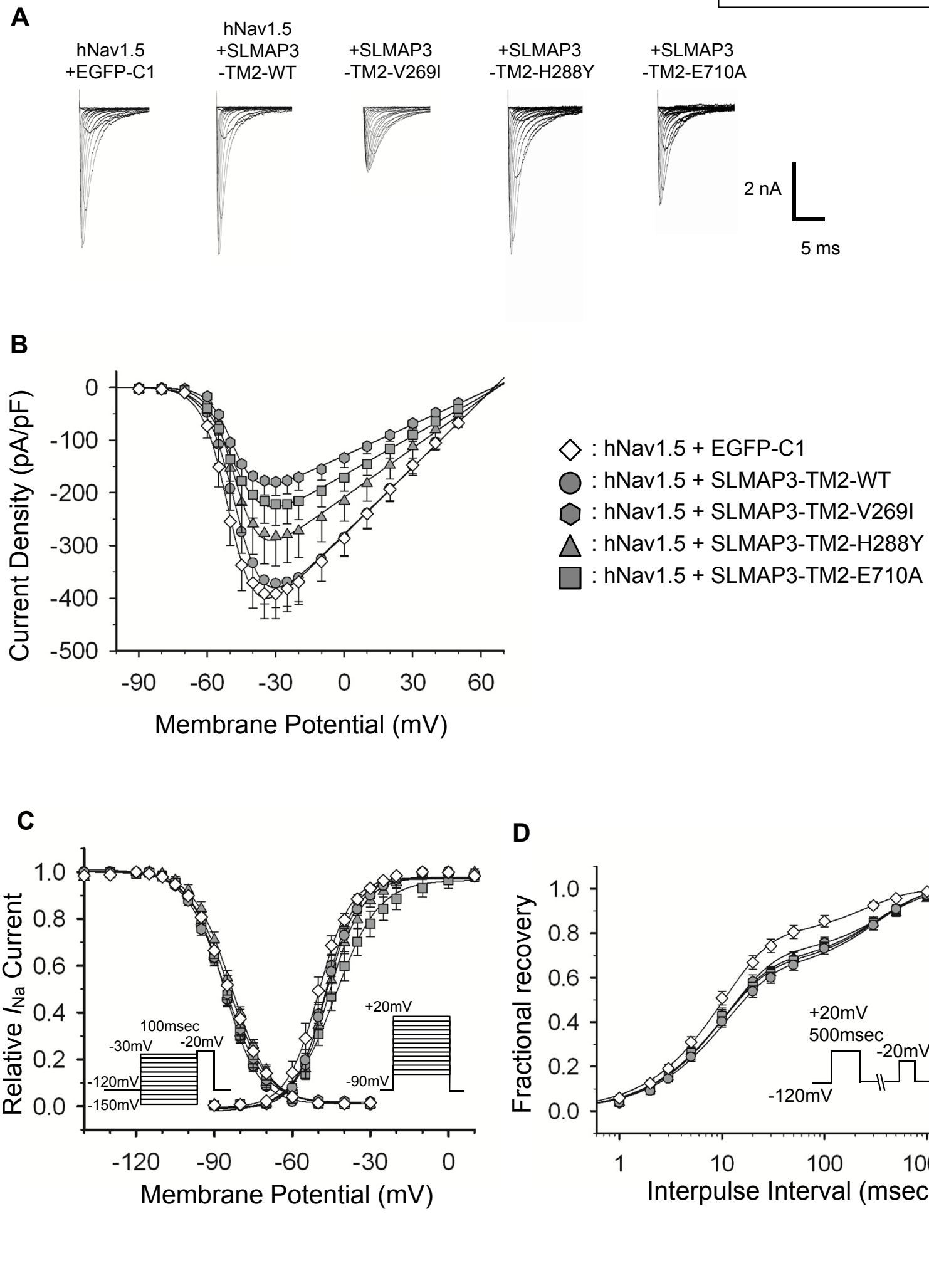

Supplemental Figure S6

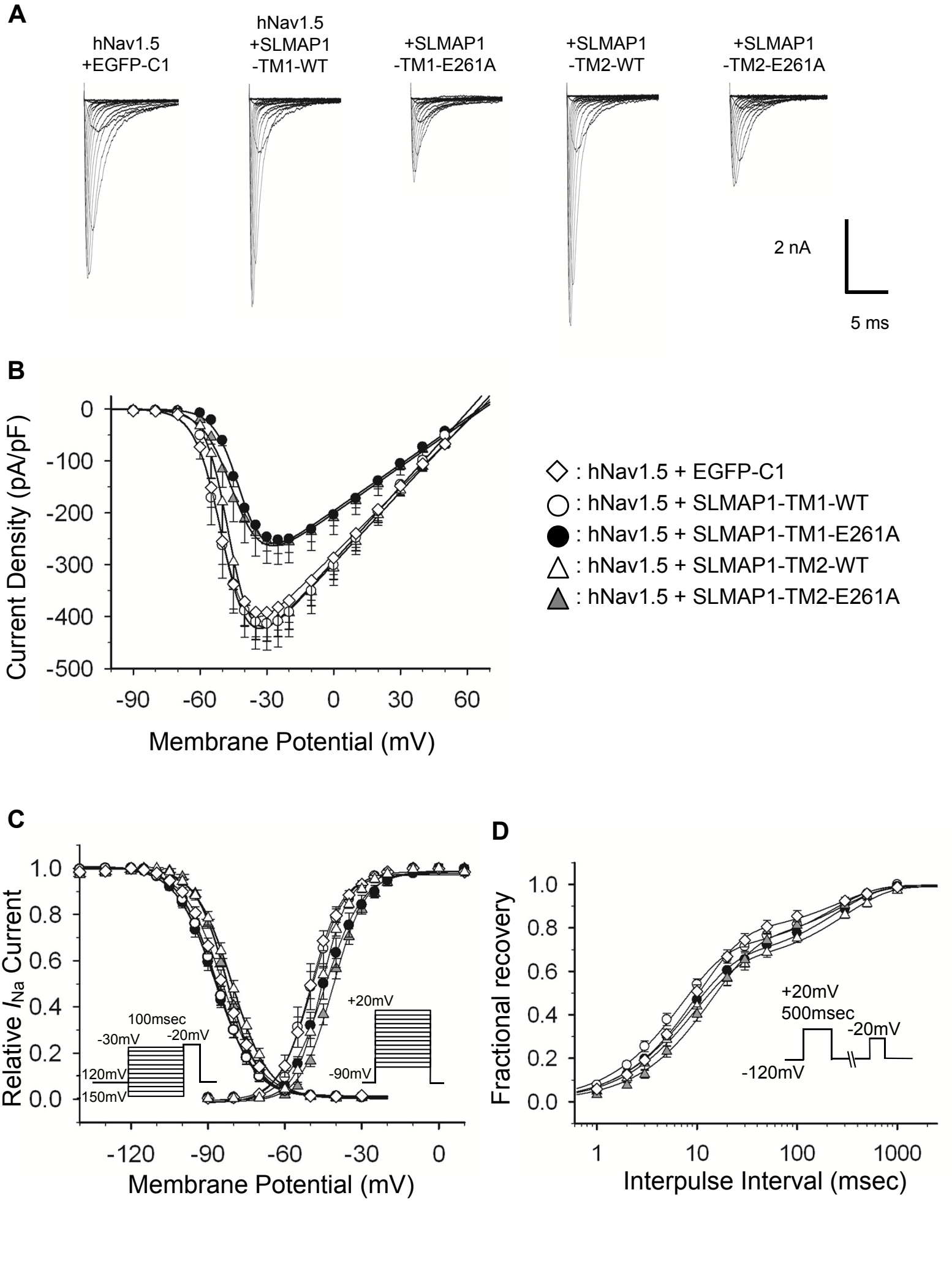

Supplemental Figure S7

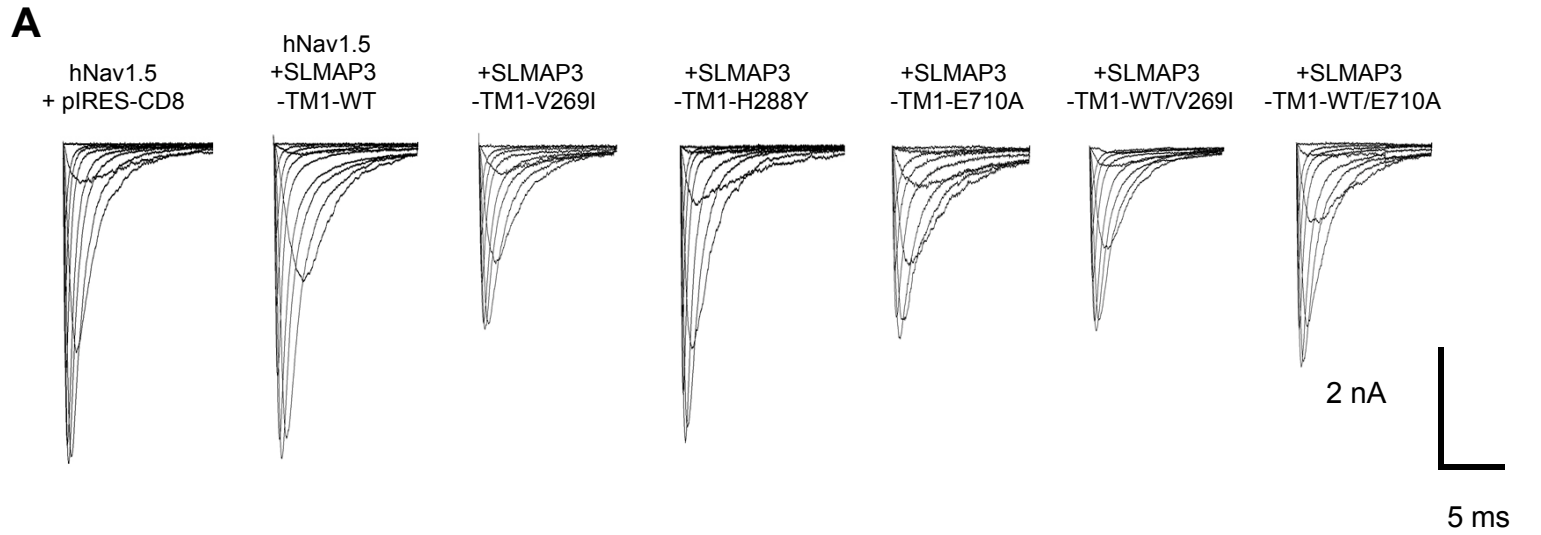

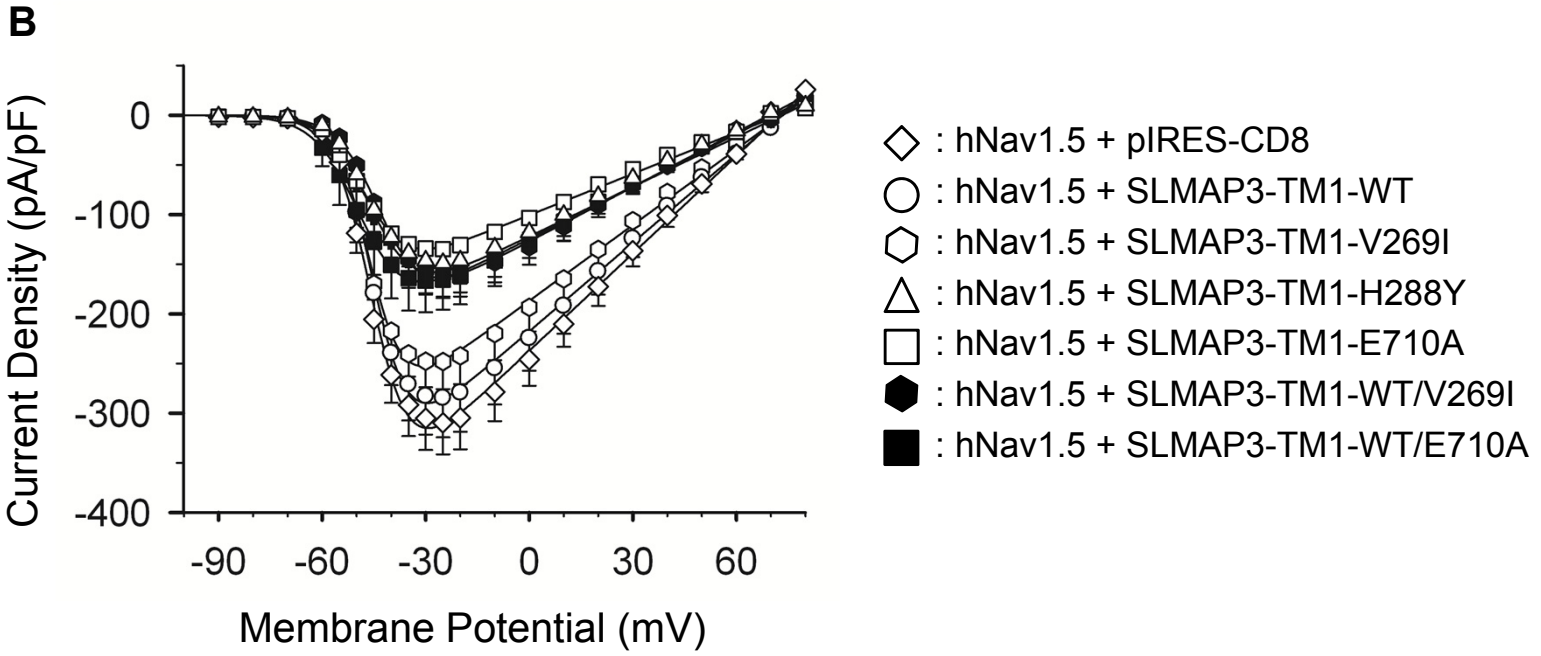

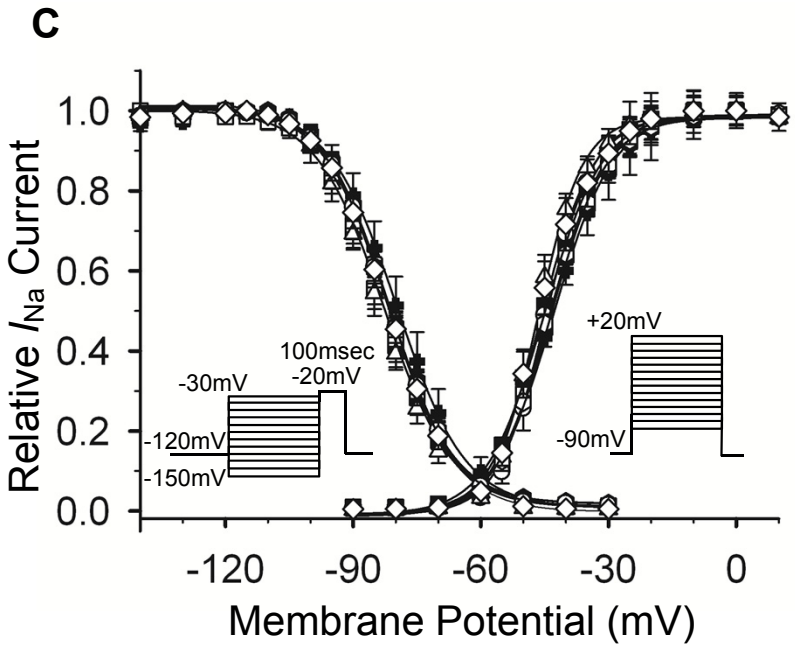

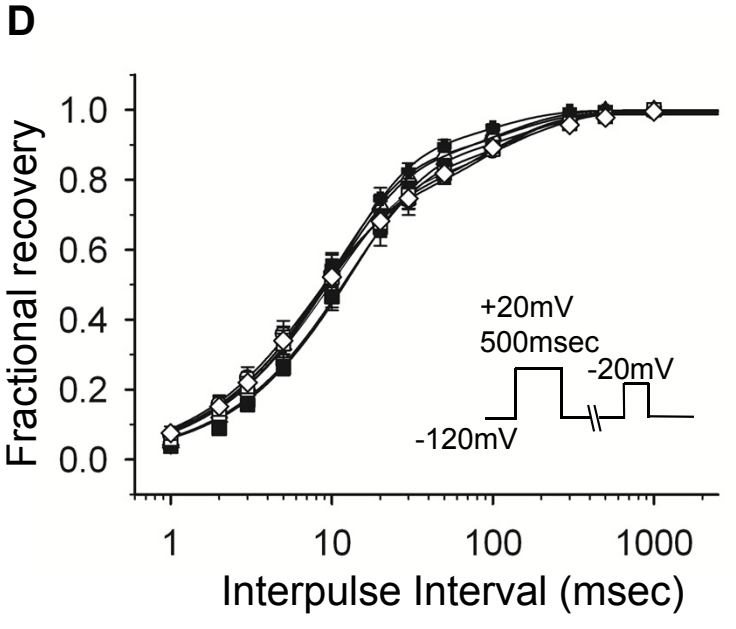

Supplemental Figure S8

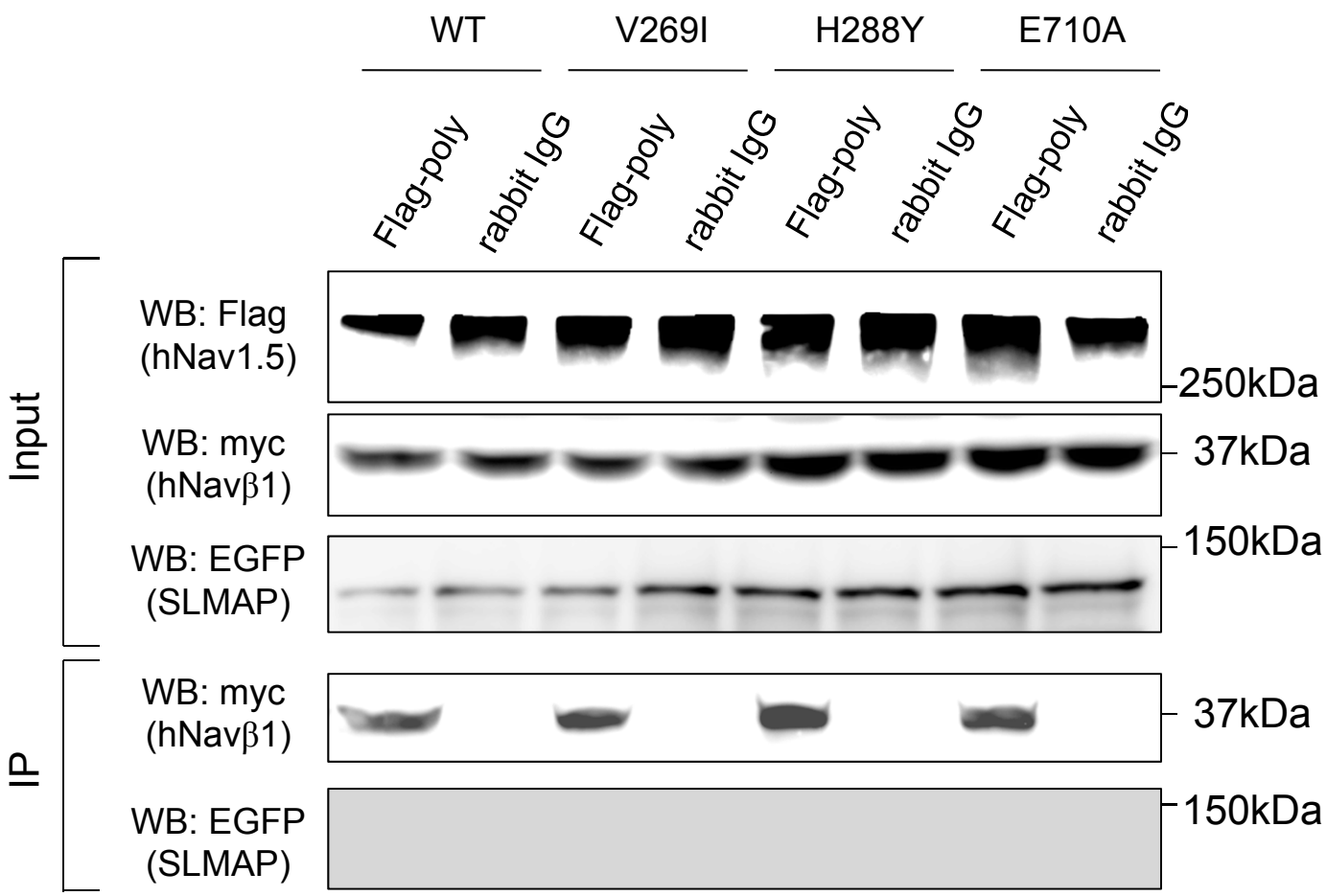

A Novel Disease Gene for Brugada Syndrome: Sarcolemmal Membrane–Associated Protein Gene Mutations Impair Intracellular Trafficking of hNav1.5

Taisuke Ishikawa, Akinori Sato, Cherisse A. Marcou, David J. Tester, Michael J. Ackerman, Lia Crotti, Peter J. Schwartz, Young Keun On, Jeong-Euy Park, Kazufumi Nakamura, Masayasu Hiraoka, Kiyoshi Nakazawa, Harumizu Sakurada, Takuro Arimura, Naomasa Makita and Akinori Kimura

Circ Arrhythm Electrophysiol. 2012;5:1098-1107; originally published online October 12, 2012;
doi: 10.1161/CIRCEP.111.969972
Circulation: Arrhythmia and Electrophysiology is published by the American Heart Association, 7272 Greenville Avenue, Dallas, TX 75231

Print ISSN: 1941-3149. Online ISSN: 1941-3084